MedChemComm

Accepted Manuscript

ROYAL SOCIETY OF CHEMISTRY

www.rsc.org/medchemcomm

Journal Name

RSCPublishing

ARTICLE

Bicyclic imidazole-4-one derivatives: a new class of antagonists for the orphan G protein-coupled receptors GPR18 and GPR55

Cite this: DOI: 10.1039/xoxxoooooox

Received ooth January 2012,
Accepted ooth January 2012

DOI: 10.1039/xoxxoooooox

www.rsc.org/

V. Rempel,[#] K. Atzler,[#] A. Behrenswerth,[#] T. Karcz,[#,§] C. Schoeder,[#] S. Hinz,[#] M. Kaleta,[§] D. Thimm,[#] K. Kiec-Kononowicz,[§] and C. E. Müller[#,*]

GPR18 and GPR55 are orphan G protein-coupled receptors (GPCRs) that interact with certain cannabinoid (CB) receptor ligands. In the present study bicyclic imidazole-4-one derivatives were discovered as new scaffolds for the development of antagonists for GPR18 and GPR55. Interaction with CB_1 and CB_2 receptors was also studied to assess selectivity. The presented extensive structure-activity relationship study of 49 derivatives investigated at all four GPCRs revealed structural requirements for the development of potent and selective GPR18 and GPR55 antagonists. (*Z*)-(2,3-difluorobenzylidene)-6,7-dihydro-2*H*-imidazo[2,1-*b*][1,3]thiazin-3(5*H*)-one (**18**) was identified as a selective GPR55 antagonist (IC_{50} 3.15 µM). The most potent GPR18 antagonist was **(***Z***)**-2-(3-(4-chlorobenzyloxy)benzylidene)-6,7-dihydro-2*H*-imidazo[2,1-*b*][1,3]thiazin-3(5*H*)-one (**32**, IC_{50} 0.279 µM, >36-fold selective vs. CB_1 and GPR55, 14-fold selective vs. CB_2) representing the first selective GPR18 antagonist. The new compounds may serve as lead structures and as tools to explore the (patho-)physiological roles of these orphan GPCRs and their potential as drug targets.

Introduction

Two distinct cannabinoid (CB) receptor subtypes are known to date, designated CB_1 and CB_2, which belong to the G protein-coupled receptor (GPCR) superfamily of 7-transmembrane receptors.[1] Together with their endogenous ligands anandamide (**1**) and 2-arachidonoylglycerol (**2**), and the enzymes responsible for their production and degradation, the cannabinoid receptors are part of the endocannabinoid system, which is involved in a variety of physiological and pathophysiological processes. These include the regulation of appetite and energy homeostasis, cognitive and mental functions, and effects on pain transmission and inflammation.[2-5] Due to the immense potential of cannabinoids and CB receptor antagonists as drugs, a variety of synthetic compounds has been developed and pharmacologically characterized.[6] However, some of the pharmacological studies revealed that not all observed effects caused by cannabinoids could be fully explained by interaction of the compounds with the known CB receptors since some effects were also observed in CB receptor knock-out mice. These results indicated that certain cannabinoids are able to interact with further targets.[3, 7]

Recently the orphan receptor GPR18 was reported to be activated by Δ^9-THC (**3**) as well as by the endogenous CB receptor agonist anandamide (**1**).[8-11] Cannabidiol (**4**) was found to be a moderately potent partial agonist at GPR18, whereas its isomer, abnormal cannabidiol is a full GPR18 agonist with higher potency.[11] Like the CB receptor subtypes CB_1 and CB_2, GPR18 is coupled to G_i proteins mediating an inhibition of adenylate cyclase.[12] Furthermore, mitogen-activated protein (MAP) kinase activation was reported.[13]

So far, very little is known about the (patho)physiological roles of GPR18. Studies have shown that it is highly expressed in testes, spleen, endometrium and metastatic melanoma cells, and at lower levels in thymus and in peripheral white blood cells.[8, 13, 14] Due to its distribution GPR18 is thought to be involved in maintaining tumor cell survival, e.g. of melanoma cells, and to modulate immune functions.[8, 14] In addition, activation of GPR18 was reported to induce migration of human endometrial cells.[10] Thus GPR18 antagonists may be useful novel therapeutics for the treatment of endometriosis and cancer.

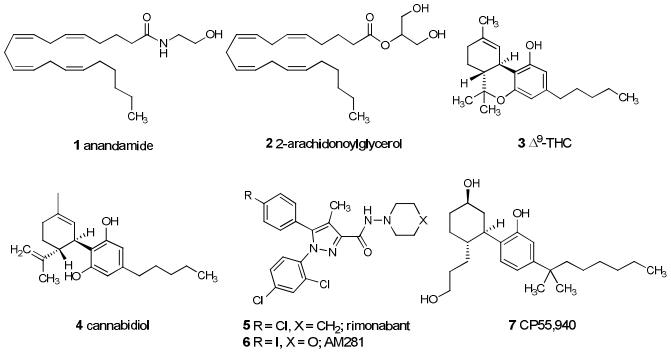

Figure 1. Structures of selected cannabinoids and CB receptor ligands reported to interact with GPR18 and/or GPR55

The orphan GPCR GPR55 is another receptor which has been found to be activated by certain CB receptor ligands, including the CB_1 inverse agonist rimonabant (**5**), and inhibited by others, such as

the CB receptor agonist CP55,940 (**7**).[7, 15, 16] GPR55 activation leads to $G_{12/13}$ protein-mediated formation of RhoA, which in turn activates phospholipase C via Rho kinase (ROCK) resulting in a subsequent release of Ca^{2+} from intracellular stores.[17] GPR55 is highy expressed in adrenal glands, the central nervous system, certain cancer cell lines and immune cells as well as osteoclasts and osteoblasts.[16, 18-20] The receptor has been postulated to play a role in mediating inflammatory and neuropathic pain, in promoting cancer cell migration and proliferation, and in the regulation of bone mass.[18, 21, 22] GPR55 receptor antagonists are therefore considered as potential drug candidates for the treatment of cancer, neuropathic pain and osteoporosis.[2, 18, 21, 22]

Despite their interaction with several CB receptor ligands, GPR18 and GPR55 are not closely related to the classical CB receptors. Their reported endogenous agonists *N*-arachidonoylglycine (NAGly, **8**, for GPR18), an anandamide metabolite, and 1-lysophosphatidylinositol (**9**, for GPR55) are inactive at CB_1 and CB_2 receptors.[2, 11, 22-24] In addition, studies investigating an interaction of the endocannabinoids anandamide (**1**) and 2-arachidonoylglycerol (**2**) with GPR18 and GPR55 are inconsistent. McHugh et al. reported on an activation of GPR18 by anandamide (**1**), and several research groups described anandamide (**1**) and 2-arachidonoylglycerol (**2**) as agonists at GPR55.[11, 23] But those results could not be confirmed by other groups.[7, 22, 25, 26] Furthermore, the degree of sequence identity between CB receptors and GPR18 (identity to CB_1 12%, to CB_2 7%), and CB receptors and GPR55 (identity to CB_1 15%, CB_2 to 13%) is relatively low, compared to an identity of 44% between both CB receptor subtypes.

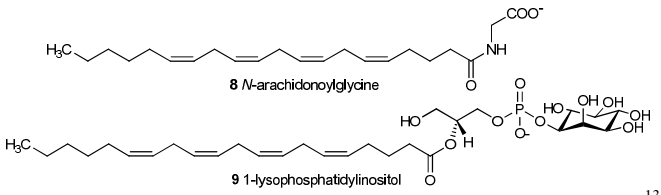

Figure 2. Postulated endogenous agonists at GPR18 (NAGly, **8**)[13] and GPR55 (LPI, **9**)[22]

The development of potent and selective ligands for GPR18 and GPR55 is required to further study the receptors' role in health and disease, and to explore their potential as drug targets.[15, 22] In particular, antagonists for GPR18 and GPR55 are urgently needed research tools. So far only two studies reported the development of selective GPR55 receptor antagonists,[27, 28] and to the best of our knowledge no selective GPR18 antagonists have so far been described. In addition, it is important to investigate established and new CB receptor ligands for their potential interaction with GPR18 and GPR55, since some of the (adverse) effects of CB receptor ligands may be actually mediated by interaction with the orphan receptors GPR18 and/or GPR55.

Neither for the orphan GPCRs GPR18 and GPR55, nor for the CB receptors, crystal structures have been determined yet. Thus, screening campaigns, followed by structure-activity relationship (SAR) studies currently appear to be the most promising approach to identify new ligands for the poorly characterized orphan receptors GPR18 and GPR55. Therefore we screened part of our proprietary compound library focusing on lipophilic structures (http://www.pharma.uni-bonn.de/www/pharmchem1/mueller-laboratory/compound-library?set_language=en). By performing β-arrestin translocation, and cAMP accumulation assays, respectively, we identified new lead structures for GPR18 and GPR55, as well as for CB_1 and CB_2 receptors, and subsequently optimized them for the new target receptors. Our study provides SARs of a series of 49 synthesized compounds at all four CB and CB-like receptors, and thus enables new insights into the structural requirements to selectively address each of these promising drug targets.

Results and Discussion

Syntheses

The target compounds were synthesized starting from *Z*-5-arylidene-2-thiohydantoin, or from 5,5-diphenyl-2-thiohydantoin, respectively, by previously developed methods.[29-38] 5-Arylidene-2-thiohydantoins were obtained by Knoevenagel condensation of aldehydes or ketones with 2-thiohydantoin (methods A-C).

Scheme 1. Synthesis of arylidene-imidazo[2,1-*b*]thiazine and -imidazo[2,1-*b*]thiazepine derivatives[a]

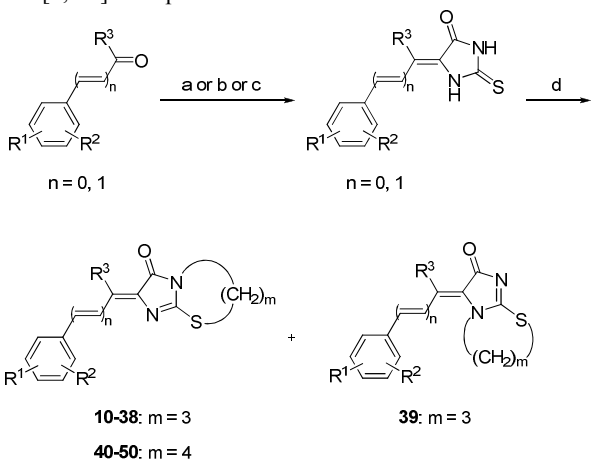

[a]Reagents and conditions: (a) 2-thiohydantoin, alanine, Na_2CO_3, water, reflux; (b) 2-thiohydantoin, sodium acetate, acetic acid, reflux; (c) 2-thiohydantoin, ammonium acetate, toluene, reflux; (d) $Br(CH_2)_mBr$, BTEA, K_2CO_3, acetone, rt.

Cyclization of 2-thiohydantoin derivatives with dibromopropane or dibromobutane under phase-transfer catalysis in acetone, in the presence of potassium carbonate and benzyltriethylammonium chloride (BTEA) as a catalyst, provided the desired *Z*-7-arylideneimidazo[2.1-*b*]thiazines **10-39** and the *Z*-8-arylidene-imidazo[2.1-*b*]thiazepines **40-50**. *Z*-7-arylideneimidazo[2.1-*b*]-thiazines were prepared by 1,2- (**39**) or 2,3- (**10-38**) cyclization of the starting 2-thiohydantoin derivatives (Scheme 1). All described arylidene derivatives were obtained as *Z*-configurated stereoisomers as confirmed for several examples by X-ray structure analysis. According to our extensive experience with this class of compounds, the arylidene double bond is not reactive towards nucleophiles, which can be explained by its conjugation with the ring system.

5,5-Diphenyl-2-thiohydantoin was alkylated with dibromoalkanes (dibromoethane for **51** and **53**, **55** and **56**, dibromobutane for **57** and **58**, or ethyl 2,3-dibromopropionate for **52** and **54**) to yield the products of 1,2- (**51**, **52**, **55**, **57**) or 2,3- (**53**, **54**, **56**, **58**) cyclization as depicted in Scheme 2.

Scheme 2. Synthesis of diphenyl-imidazo[2,1-*b*]thiazole, -imidazo-[2,1-*b*]thiazine and -imidazo[2,1-*b*]thiazepine derivatives[a]

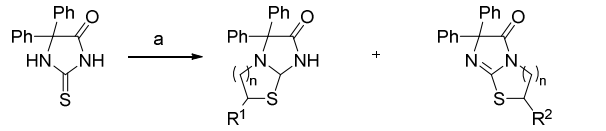

51: n = 1 R^1 = H
52: n = 1 R^1 = COOEt
55: n = 2 R^1 = H
57: n = 3 R^1 = H

53: n = 1 R^2 = H
54: n = 1 R^2 = COOEt
56: n = 2 R^2 = H
58: n = 3 R^2 = H

[a]Reagents and conditions: (a) $BrCH_2CH(Br)COOEt$ or $Br(CH_2)_nBr$, BTEA, K_2CO_3, acetone, rt.

The obtained compounds were purified by column chromatography. Their structures were confirmed by spectral analyses including IR, ^{1}H-NMR, ^{13}C NMR, and ESI-MS spectra. Purity was confirmed by TLC, LC-MS and elemental analyses (for details see Experimental Section and Supplementary Materials).

Biological Evaluation

Imidazo[2,1-*b*]thiazole (**51**, **52**, **53, 54**), imidazo[2,1-*b*]thiazine (**10-39**, **55, 56**) and imidazo[2,1-*b*]thiazepine (**57**, **58**, **40-50**) derivatives were investigated in order to assess their potential to interact with the orphan receptors GPR18 and GPR55, as well as with the two established CB receptor subtypes CB_1 and CB_2, and to study their SARs. Due to the lack of potent radioligands for the orphan receptors GPR18 and GPR55 an interaction of the compounds with these receptors was determined in β-arrestin translocation assays based on the β-galactosidase enzyme fragment complementation technology (β-arrestin PathHunter™ assay, DiscoverX, Fremont, CA, USA). This assay format has been shown to be very useful for the investigation of orphan receptors.[26, 28, 39-41] The measured luminescence signal is specific for the investigated receptor in a recombinant cell line (Chinese hamster ovary cells) stably expressing the respective human GPCR, since artefacts due to activation of endogenous receptors can be excluded.[26] For additional confirmation of signal specificity, a small subset of compounds was additionally tested at the human GPR35 using the same technology. The compounds were initially screened for agonistic and antagonistic activity at a concentration of 10 µM. Screening for antagonistic activity was performed by preincubation of the cells with test compound followed by stimulation with a standard agonist (GPR18: Δ^9-THC, 10 µM, corresponding to its EC_{90}; GPR55: LPI, 1 µM, corresponding to its EC_{50}; GPR35: zaprinast, 5 µM, corresponding to its EC_{80}).[39, 42] IC_{50} and/or K_B values were determined for compounds showing an inhibition of >60 % of the effect produced by the standard agonist under the conditions described above. To investigate the affinity of the compounds for CB receptors, radioligand binding assays were performed at recombinant human CB_1 and CB_2 receptors stably expressed in CHO, or HEK293 (human embryonic kidney) cells, respectively. Most of the compounds were additionally tested at native rat CB_1 receptors in rat brain cortical membrane preparations. [^{3}H](-)-*cis*-3-[2-Hydroxy-4-(1,1-dimethylheptyl)phenyl]-*trans*-4-(3-hydroxypropyl)cyclohexanol ([^{3}H]CP55,940, **7**) was utilized as a CB_1 and CB_2 radioligand. Initially, the compounds were screened at a concentration of 10 µM. In cases were inhibition of radioligand binding was greater than 50%, full concentration-inhibition curves were determined in order to calculate K_i values. The most potent compounds of the present series were investigated for their functional properties in cAMP accumulation assays using CHO cells stably expressing the human CB_1 or CB_2 receptor subtype. In addition, [^{35}S]GTPγS binding assays were conducted as a measure of receptor activation at rat brain cortical membranes, and at HEK cells stably expressing the human CB_1, or CB_2 receptor subtype, respectively. Since some members of the investigated class of compounds had previously been found to interact with the benzodiazepine binding site of rat brain $GABA_A$ receptors[29] we performed binding studies for selected potent compounds versus [^{3}H]diazepam as previously described[29] to assess their selectivity (see Supplementary Materials, Table S3).

Structure-activity relationships

Antagonistic potencies of the compounds at GPR18 and GPR55 are collected in Table 1, along with their binding affinities at CB_1 and CB_2 receptors. For direct comparison, Table 1 also contains test results of standard ligands obtained in our laboratory under the same conditions. These include Δ^9-THC (**3**, (partial) agonist at GPR18, CB_1 and CB_2) *N*-arachidonoylglycine (NAGly, **8**, reported GPR18 agonist), LPI (**9**, agonist at GPR55), rimonabant (**5**, antagonist at GPR18; agonist at GPR55; inverse agonist at CB_1), and CP55,940 (**7**, antagonist at GPR18 and GPR55, agonist at CB_1 and CB_2).[10, 12, 13, 15, 16] Comparison of IC_{50} values obtained form β-arrestin assays (GPR18, GPR55) with K_i values from radioligand binding studies (CB_1, CB_2) will provide a rough estimate of the compounds' selectivity.

We could confirm that Δ^9-THC (**3**) behaves as a GPR18 agonist in β-arrestin recruitment assays.[28] The obtained EC_{50} value of 4.61 µM is consistent with literature data (EC_{50} of 0.96 µM) determined in a MAP kinase assay in HEK293 cells stably expressing GPR18.[11] However, the second reported GPR18 agonist, NAGly (**8**), failed to activate GPR18 in our test system. Our results support the recent findings of two other groups which also failed to observe activation of GPR18 by NAGly in several assay systems.[26, 27] Thus, further investigations are required to reveal the true role of NAGly in GPR18-mediated signalling. The non-selective CB agonist CP55,940 (**7**) and the CB_1-selective inverse agonist rimonabant (**5**) displayed antagonistic activities at GPR18 with potencies in the low micromolar concentration range.[28] In agreement with literature data, we could confirm that CP55,940 (**7**) and rimonabant (**5**) also interact with GPR55,[7, 15, 16, 40] rimonabant (**5**) being an agonist (EC_{50} 2.01 µM), while CP55,940 (**7**) was shown to be an antagonist at GPR55 (IC_{50} 1.61 µM).[40] Like **7**, Δ^9-THC also behaved as an antagonist at GPR55.[28] The determined affinities of the standard cannabinoids at CB receptors are consistent with published data.[43]

In the newly investigated series of bicyclic imidazole-4-ones, compounds with selectivity for either GPR18 or GPR55, or for CB_1 receptors, respectively, were discovered. Almost all of the potent compounds behaved as antagonists or inverse agonists at the respective receptor. The imidazo[2,1-*b*]thiazine (A) and the imidazo[2,1-*b*]thiazepine (C) scaffolds were found to be suitable for the development of GPR18 antagonists, imidazo[2,1-*b*]thiazines (A) generally displaying higher potency as compared to the analogous imidazo[2,1-*b*]thiazepines (C) (compare **31** and **42**, **32** and **43**, **33** and **45**, **34** and **46**). The potency of the compounds at GPR18 correlated with the size of the residues in position 2 of the annelated heterocycle: while *Z*-benzylidene-substituted imidazo[2,1-*b*]thiazines (**R** = (substituted) phenyl, **10-29**) failed to interact with GPR18, bulky biaromatic residues such as *m*-benzyloxybenzylidene (**31**, GPR18 IC_{50} 7.22 µM)) and *m*-benzoyloxybenzylidene (**36**, GPR18 IC_{50} 6.35 µM) led to a remarkable increase in inhibitory potency. Introduction of chlorine atoms at the benzyloxybenzylidene residue further enhanced potency of the compounds, especially in the imidazothiazine series A (compare **31** with **32-35**) and in some cases had a great impact on selectivity. Introduction of a *p*-chloro-

substituted benzyloxy residue (**32**), for instance, shifted the affinity towards GPR18 (GPR18 IC_{50} 0.279 μM, no interaction with GPR55 and CB_1, K_i CB_2 4.03 μM,), while an *o,p*-dichloro-substituted benzyloxy moiety (**34**) enhanced affinity for CB_1 and CB_2 (GPR18 IC_{50} 2.55 μM, K_i CB_1 2.09 μM, K_i CB_2 0.95 μM, no interaction with GPR55). *o*-Chloro- (**33**) and *m,p*-dichloro- (**35**) substituted benzyloxy-substituted derivatives displayed no affinity for CB receptors, but considerable potency at GPR18 (**33**, GPR18 IC_{50} 1.65 μM; **35**, GPR18 IC_{50} 6.16 μM). Although the *o*-chloro- (**33**, GPR18 IC_{50} 1.65 μM) and the *p*-chloro- (**32**, GPR18 IC_{50} 0.279 μM) derivatives were the most potent GPR18 antagonists of the present series, the combination realized in the *o,p*-dichloro derivative **34** was not additive (GPR18 IC_{50} 2.55 μM). Displacement of the (*p*-chloro)benzyloxy (**31**, **32**) by a (*p*-chloro)benzoyloxy (**36, 37**) residue decreased affinity at CB_1 and CB_2 receptors, while the substitution was tolerated by GPR18, although reduced potency was observed in the case of the chlorinated compound **37**. However, it cannot be completely ruled out that the ester function might be partly hydrolyzed by esterases potentially present on the cell surface of the utilized CHO cells. The *p*-chlorobenzyloxybenzylidene-substituted imidazothiazine derivative **32** was the most potent GPR18 antagonist of the present series displaying an IC_{50} value of 0.279 μM, >>36-fold selectivity over CB_1 and GPR55, and 14-fold selectivity over CB_2 receptors. In the imidazothiazepine series C only the introduction of an *ortho*- (**45**) but not a *para*-chloro substituent increased potency at GPR18 (**43**, compare to the unsubstituted benzyloxybenzylidene derivative **42**). If the imidazothiazinone scaffold was substituted by smaller fluoro-, chloro-, or methoxy-benzylidene moieties instead of larger aromatic residues, potent GPR55 ligands could be obtained. Especially *ortho*-halogen (Cl, F) substitution led to an increase in inhibitory potency at GPR55. The most potent compounds of the series were the *o,m*-difluorobenzylidene derivative **18** (GPR55 IC_{50} 3.15 μM), the *o,p*-difluorobenzylidene derivative **19** (GPR55 IC_{50} 3.46 μM), and the *o*-chloro-benzylidene derivative **13** (GPR55 IC_{50} 5.09 μM), while the methoxy-substituted benzylidene derivatives were less potent at GPR55, the best one being the *o,p*-dimethoxybenzylidene derivative **27** (GPR55 IC_{50} 9.77 μM). As nearly all of the benzylidene-substituted imidazo[2,1-*b*]thiazines possessed no or only low affinities for GPR18 and CB receptors, they represent promising lead structures for the future development of more potent and selective GPR55 ligands. It appears that the GPR55 prefers smaller ligands, while GPR18 as well as the CB receptors require larger, more lipophilic, lipid-like ligands, at least with respect to the present series of compounds.

Introduction of larger residues containing two aromatic rings as in imidazothiazines (A) **30-37** and in imidazothiazepines (C) **40-47** reduced the inhibitory potency of the compounds at GPR55. Except for **35** (IC_{50} 11.8 μM) none of the compounds of this subgroup displayed notable inhibition of GPR55. Our current findings are consistent with previous observations made in a different series of GPR55 antagonists based on a coumarin scaffold indicating that large, lipophilic residues were not required for high inhibitory potency at the LPI-activated GPR55, and selectivity versus the CB receptor subtypes including GPR18 can easily be reached.[28] Interestingly, the *p*-chlorobenzyloxybenzylidene-substituted imidazothiazepinone **43** behaved as a moderately potent agonist at GPR55 (EC_{50} 10.7 μM). However, **43** showed much higher affinity for CB receptors, especially for the CB_1 subtype (K_i CB_1 0.25 μM).

Compounds with notable CB receptor affinity were identified among those members of series A (**27**, **30-32**, **34**) and C (**40-47**, **49**), which contained large substituents mostly consisting of two connected aromatic rings, as well as in the diphenyl-substituted series F (**58**). It became evident that affinity of 5,5-diphenylimidazol-4-one derivatives (**51-58**) to CB receptors depended on the size of the heterocycle annelated to the imidazole ring. While imidazo-[2,1-*b*]thiazole derivatives (**51-54**) and the thiazine derivatives **55** and **56** displayed no or very low affinity to CB receptors, thiazepine derivatives, in particular **58**, showed increased affinity for the CB_1 receptor. Due to the synthetic pathway two isomeric products were obtained: 1,2-substituted (series F) and 2,3-substituted imidazoles (series E).[34] The two isomeric series differed in their affinity for CB_1 receptors. The most potent compound of the 5,5-diphenylimidazol-4-one series, **58** (series F) containing a thiazepine ring showed a K_i value of 1.34 μM at human CB_1 receptors and was selective versus the CB_2 receptor, GPR18 and GPR55. Displacement of the 5,5-diphenyl moiety by *Z*-benzylidene residues containing small substituents (**10-29**) or an (*E,E*)-phenylbutadienyl residue (**38** and **39**) generally reduced the affinity of the compounds for CB receptors. However, by introduction of large, lipophilic residues, such as unsubstituted or halogen-substituted *m*-benzyloxy-benzylidene residues (**31**, **32**, and **42-47**) CB receptor affinity was increased. Compounds with high CB receptor affinity, some of which showed selectivity for CB_1 (e.g. **43** K_i CB_1 0.25 μM, K_i CB_2 4.15 μM), could thus be obtained.

Most compounds were additionally tested in radioligand binding assays at native CB_1 receptors in rat brain cortical membrane preparations (see Supplementary Information Table S1). Species differences were found to be moderate, and apart from few exceptions K_i values were comparable in both species. Exceptions included **30-32** and **56** with somewhat higher affinity for rat than for human CB_1, and **45**, **48** with higher affinity for human than for rat CB_1 receptors (see Table S1).

Our results revealed that compounds of the presented series with high affinity at CB receptors in most cases also interacted with

Table 1. Affinities and potencies of annelated imidazolone derivatives at GPR18, GPR55, CB_1 and CB_2 receptors[a]

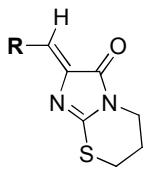
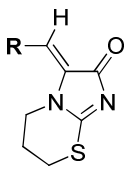
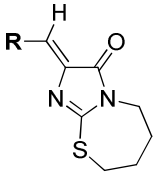
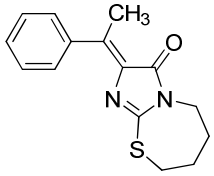
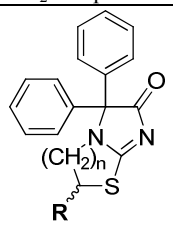
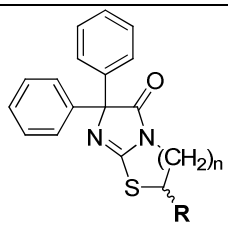

A	**B**	**C**	**D**	**E**	**F**
10-38	**39**	**40-49**	**50**	**51**, **52**, **55**, **57**	**53**, **54**, **56**, **58**
		β-arrestin recruitment assay		radioligand binding assays vs. [^{3}H]CP55,940	

compd	**R**	**human GPR18** IC_{50} ± SEM[a] (μM) (% of Δ^9-THC inhibition)[b]	**human GPR55** IC_{50} ±SEM[a] (μM) (% of LPI inhibition)[c]	**human CB_1** K_i ± SEM[a] (μM) (% inhibition)[d]	**human CB_2** K_i ± SEM[a] (μM) (% inhibition)[d]
Standard ligands					
3	See figure 1	*agonist* **EC_{50} 4.61**[28]	**14.2**[28]	**0.00388** ± 0.00091	**0.0716** ± 0.0024
5	See figure 1	**10.1**[28]	*agonist* **EC_{50} 2.01**[40]	**0.0126**[44]	**0.900**[44]
7	See figure 1	**5.99**[28]	**1.61**[40]	**0.00128**[44]	**0.00142**[44]
8	See figure 2	>10 (0%)	>10 (6%)	>10 (43%)	>10 (36%)
9	See figure 2	>10 (15%)	*agonist* **EC_{50} 1.00**[40]	>10 (0%)	>10 (0%)
Imidazo[2,1-*b*][1,3]thiazin-3-ones (A)					
10	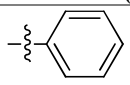	>10 (5%)	>10 (25%)	>10 (40%)	>10 (18%)
11	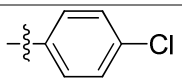	>10 (18%)	>10 (35%)	>10 (25%)	>10 (23%)
12	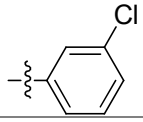	>10 (14%)	≥10 (42%)	>10 (30%)	>10 (2%)
13	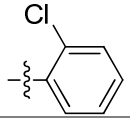	>10 (6%)	**5.09** ± 0.35	>10 (0%)	>10 (21%)
14	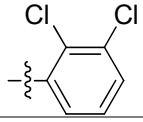	>10 (0%)	**6.91** ± 1.04	>10 (12%)	>10 (40%)

15	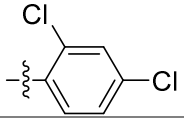	>10 (14%)	**6.76** ± 1.37	>10 (8%)	> 10 (24%)
16	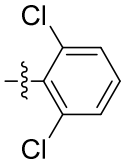	>10 (0%)	>10 (0%)	>10 (14%)	>10 (4%)
17	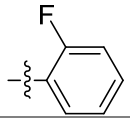	>10 (17%)	**5.56** ± 1.10	>10 (13%)	>10 (0%)
18	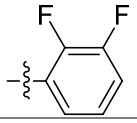	>10 (3%)	**3.15** ± 0.20	>10 (7%)	> 10 (0%)
19	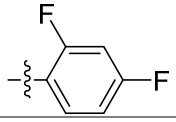	>10 (6%)	**3.46** ± 1.34	>10 (13%)	> 10 (0%)
20	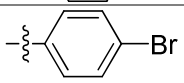	>10 (13%)	>10 (16%)	>10 (29%)	>10 (8%)
21	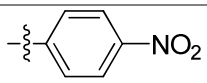	>10 (20%)	>10 (12%)	>10 (0%)	>10 (20%)
22	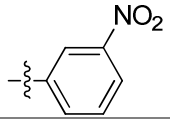	>10 (6%)	>10 (20%)	>10 (19%)	>10 (10%)
23	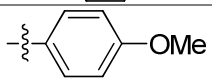	>10 (10%)	>10 (16%)	>10 (39%)	>10 (6%)
24	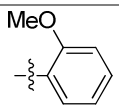	>10 (0%)	>10 (33%)	>10 (4%)	>10 (27%)
25	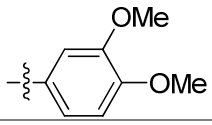	>10 (2%)	>10 (12%)	>10 (7%)	>10 (18%)
26	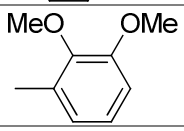	>10 (10%)	**16.4** ± 5.8	>10 (18%)	> 10 (15%)
27	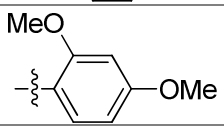	>10 (7%)	**9.77** ± 0.34	≥10 (42%)	**2.57** ± 1.09
28	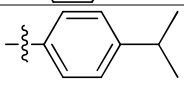	>10 (4%)	>10 (38%)	>10 (12%)	>10 (17%)

29	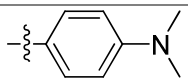	>10 (13%)	>10 (13%)	>10 (29%)	**16.6** ± 6.2
30	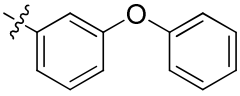	~10 (54%)	>10 (33%)	>10 (29%)	>10 (9%)
31	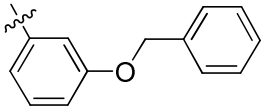	**7.22** ± 3.42	>10 (0%)	>10 (25%)	**1.11** ± 0.01
32	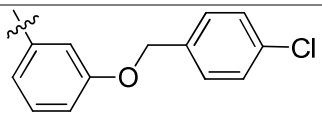	**0.279** ± 0.111	>10 (0%)	>10 (0%)	**4.03** ± 0.51
33	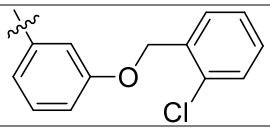	**1.65** ± 0.45	≥10 (45%)	>10 (0%)	> 10 (9%)
34	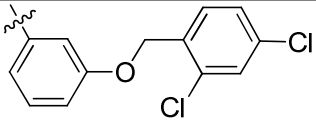	**2.55** ± 0.71	>10 (0%)	**2.09** ± 0.08	**0.95** ± 0.27
35	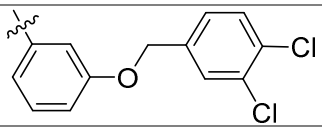	**6.16** ± 2.86	**11.8** ± 2.1	>10 (15%)	>10 (0%)
36	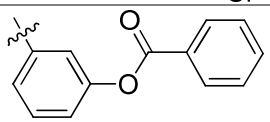	**6.35** ± 1.86	>10 (7%)	>10 (2%)	≥10 (47%)
37	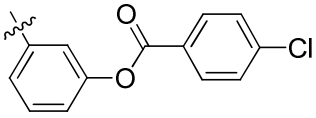	**14.3** ± 3.26	>10 (16%)	>10 (12%)	>10 (0%)
38	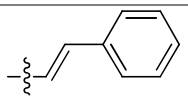	>10 (0%)	>10 (27%)	>10 (16%)	>10 (37%)
Imidazo[2,1-b][1,3]thiazin-2-ones (B)					
39	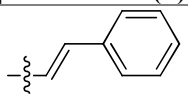	>10 (2%)	>10 (0%)	>10 (26%)	>10 (19%)
Imidazo[2,1-b][1,3]thiazepin-3-ones (C)					
40	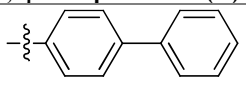	>10 (37%)	>10 (0%)	>10 (-5%)	**5.43** ± 1.31
41	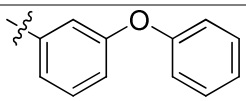	**14.1** ± 2.4	>10 (33%)	**1.60** ± 0.42	>10 (21%)

42	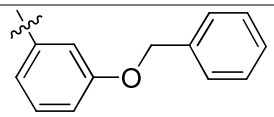	~10 (49%)	>10 (21%)	**2.13** ± 0.47	**1.81** ± 0.34
43	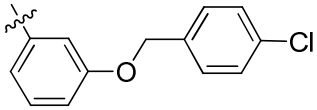	>10 (31%)	*agonist* (**EC_{50}**) **10.7** ± 0.3	**0.25** ± 0.06	**4.15** ± 0.39
44	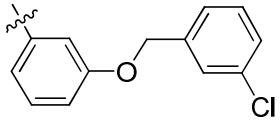	>10 (15%)	>10 (27%)	**2.16** ± 0.07	>10 (37%)
45	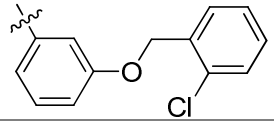	**6.48** ± 1.20	≥10 (43%)	**2.29** ± 0.46	**0.98** ± 0.23
46	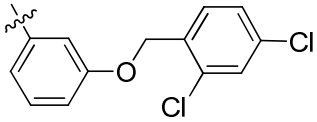	**4.61** ± 2.36	>10 (33%)	**3.18** ± 0.49	**1.65** ± 0.71
47	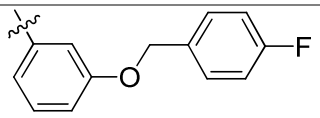	>10 (5%)	>10 (12%)	**0.85** ± 0.03	**1.56** ± 0.34
48	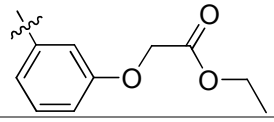	>10 (22%)	>10 (4%)	**4.78** ± 1.70	>10 (39%)
49	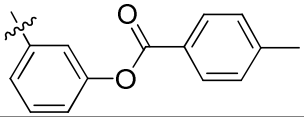	**6.45** ± 1.10	>10 (32%)	>10 (35%)	**2.58** ± 1.45
Imidazo[2,1-b][1,3]thiazepin-3-ones (D)					
50	see above for structure	>10 (4%)	>10 (25%)	>10 (10%)	>10 (17%)
Imidazo[2,1-b]thiazol-6-ones (E, n = 1)					
51	-H	>10 (0%)	>10 (31%)	>10 (30%)	>10 (6%)
52	-$COOC_2H_5$	>10 (0%)	>10 (41%)	>10 (26%)	>10 (-5%)
Imidazo[2,1-b]thiazol-5-ones (F, n = 1)					
53	-H	>10 (12%)	>10 (39%)	**21.1** ± 4.51	>10 (3%)

54	-$COOC_2H_5$	>10 (0%)	>10 (10%)	>10 (2%)	>10 (0%)
Imidazo[2,1-b][1,3]thiazin-2-ones (E, n = 2)					
55	-H	>10 (0%)	>10 (2%)	>10 (13%)	>10 (9%)
Imidazo[2,1-b][1,3]thiazin-3-ones (F, n = 2)					
56	-H	>10 (0%)	>10 (23%)	>10 (25%)	>10 (5%)
Imidazo[2,1-b][1,3]thiazepin-2-ones (E, n= 3)					
57	-H	>10 (0%)	>10 (32%)	>10 (34%)	>10 (10%)
Imidazo[2,1-b][1,3]thiazepin-3-ones (F, n=3)					
58	-H	>10 (0%)	>10 (6%)	**1.34** ± 0.37	>10 (14%)

[a]All data result from three independent experiments, performed in duplicates.
[b]Δ^9-THC was used at a concentration of 10 μM in preliminary screening assays, and at a concentration of 7.5 μM for the determination of IC_{50} values.
[c]LPI was used at a concentration of 1 μM.
[d]Percent inhibition of [^{3}H]CP55,940 binding (0.1 nM) by test compounds at a concentration of 10 μM.

GPR18, indicating that CB receptors and GPR18 require similar structural features for ligand interaction. An interaction with the established CB receptors as well as GPR18 required benzylidene residues with bulky, lipophilic substituents (**31**, **32**, **34**, **45**, **46**, **49**), while identified GPR55 ligands of the present series possessed benzylidene residues with comparably small substituents (**13**-**15**, **17**-**19**, **26**-**27**). Some compounds (e.g. **34** and **46**) blocked all three receptors, CB_1, CB_2, and GPR18 with similar potency. In particular the *o,p*-dichlorobenzyloxybenzylidene-substituted imidazothiazine derivative **34** shows inhibition of CB_1 (K_i 2.09 μM), CB_2 (K_i 0.95 μM), and GPR18 (IC_{50} 2.55 μM), and no measurable inhibition of GPR55 at 10 μM.

Interestingly an increase in affinity of the presented compounds at GPR18 and at CB receptors generally resulted in a dramatic decrease in GPR55 potency, indicating that GPR55 differs considerably in the structural features required to address its binding pocket compared to the other receptors investigated in the present study. Unfortunately, homology modelling and ligand docking is still highly speculative for the investigated group of GPCRs since no X-ray structures are currently available for any of them or for any closely related member of the class A GPCR family. Although homology models have been published based on available, distantly related GPCRs,[44-47] they do not yet appear suitable for explaining SARs and predicting optimized ligands, at least if not combined with mutagenesis studies.
In order to explore whether signals induced by the investigated compounds are specific, we tested a subset of compounds, including **10**, **13**, **18**, **27**, **32**, **43** and **44**, for their interaction (agonism or antagonism) with the GPR55-related orphan receptor GPR35. To allow for comparison we applied the same β-arrestin recruitment assay that had been used to investigate interactions with GPR18 and GPR55. All compounds were tested for agonistic as well as antagonistic activity at a concentration of 10 μM. Only compound **13** showed a moderate inhibitory effect at GPR35 (49% inhibition at 10 μM), whereas none of the other tested compounds showed any activity at the human GPR35 (see Supplementary Information, Table S2). For example, **18** (IC_{50} at GPR55 3.15 μM) was selective for GPR55 and neither interacted with GPR18 nor with GPR35 in the same test system (β-arrestin translocation using the β-galactosidase complementation assay). Also, the most potent GPR18 antagonist of the present series, compound **32**, was totally inactive at GPR35. Therefore, a specific mode of action for the presented series at the investigated GPCRs can be assumed.

Selected compounds (**12**, **13**, **18**, **19**, **32**, **34**, **36**, **43**, and **46**) were additionally investigated for their interaction with the benzodiazepine binding site of $GABA_A$ receptors at a test concentration of 10 μM (see Supplementary Information, Table S3). Only compound **13** showed significant affinity (K_i 4.15 μM), while all other investigated compounds lacked interaction or showed only low affinity. Thus, their selectivity could be confirmed including those of the GPR55 antagonist **18** and the GPR18 antagonist **32**.

Functional properties of bicyclic imidazole-4-one derivatives at GPR18 and GPR55

All compounds of the presented series were not only screened for antagonistic but also for agonistic activity at GPR18 and GPR55 in β-arrestin assays (see Supplementary Information, Table S3). For GPR18 only antagonistic screening assays revealed hits, which were

further investigated to determine IC_{50} values using various concentrations of the test compounds. The GPR18 agonist Δ^9-THC was used in a fixed concentration of 7.5 µM and inhibition of the agonist-induced signal was observed. Nine potent GPR18 antagonists were identified, of which compound **32** was the most potent one, displaying an IC_{50} value of 0.279 µM when tested versus 7.5 µM THC (corresponding to the EC_{80} of THC) (Figure 3A). As depicted in Figure 3A the THC-effect could not be fully inhibited by **32**. This is most likely due to the moderate solubility of **32**, leading to precipitation at high concentrations. Another explanation could be that **32** is an allosteric antagonist at GPR18. The inhibitory potency of compound **32** was further confirmed in assays determining concentration-response curves of the agonist Δ^9-THC in the absence and in the presence of a fixed concentration of **32** (3 µM, Figure 3B). Antagonist **32** induced a parallel rightward shift of the concentration-response curve of THC, and a pA_2 value of 1.03 µM could be determined, which was in the same range as its IC_{50} value, indicating a competitive mechanism of action.

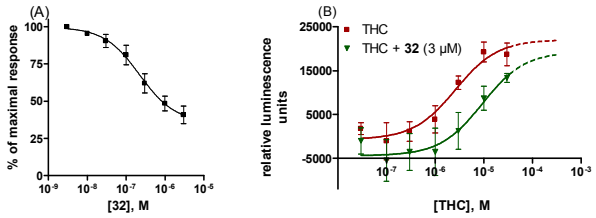

Figure 3. (A) Concentration-dependent inhibition of Δ^9-THC-induced β-arrestin recruitment to GPR18 by **32**. Δ^9-THC was used at a concentration of 7.5 µM. An IC_{50} value of 0.279 ± 0.111 µM was determined for **32**. (B) Concentration-dependent LPI response in the absence (EC_{50} 2.11 ± 0.12 µM) and in the presence of **32** (3 µM) (EC_{50} 8.54 ± 0.71). A pA_2 value of 1.03 ± 0.17 µM was calculated. Data are expressed as means ± SEM of four separate experiments performed in duplicates.

Among the compounds that were active at the human GPR55, one agonist (**43**) as well as antagonists, such as the selective compounds **18** (IC_{50} 3.15 µM, Figure 4A) and **19** (IC_{50} 3.46 µM, Figure 4B) were identified. Compounds **18** and **19** completely inhibited LPI- (1 µM) -induced receptor activation. At high concentrations of 10 µM and 30 µM, respectively, **18** and **19** decreased receptor activity even below basal values, indicating inverse agonism. Another explanation would be that the orphan GPR55 is already activated to a certain extent by natural agonists that might be present in the assay solution causing basal activation.

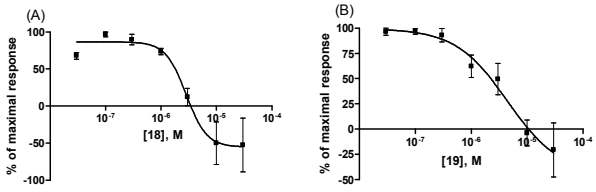

Figure 4. Concentration-dependent inhibition of LPI- (1 µM) -induced GPR55-mediated β-arrestin recruitment by (A) **18** (IC_{50}, 3.15 ± 0.20 µM), and (B) **19** (IC_{50}, 3.46 ± 1.34 µM). Data represent means of three independent experiments performed in duplicates.

Recently published studies indicated that an allosteric binding site for cannabinoid-related compounds may be present on GPR55.[23, 28] To investigate whether the identified antagonists of the present series are targeting an allosteric binding pocket different from the LPI binding site, we performed concentration-response curves for the agonist LPI in the absence and presence of antagonist (10 µM). The results for GPR55 antagonists **13**, **14**, **18** and **19** are presented in Figure 5. At a high concentration of 10 µM all compounds led to a rightward shift and at the same time to a remarkable depression of the maximal effect of the agonist-resonse curve, thus indicating allosteric antagonism. In addition, all compounds led to a reduction of basal receptor activity, which is an indication that they may be antagonists with inverse agonistic activity. Thus, the investigated compounds may be characterized as allosteric inverse agonists. Compounds bearing chloro-substituted benzylidene residues (**13**, **14**) led to a stronger depression of agonist efficacy, but were less potent than the investigated fluoro-benzylidene-substituted compounds **18** and **19** (Figure 5 and Table 1). Since the experiments require a long incubation time of 3.5 h for the antagonists (1 h of preincubation), and 2.5 h for the agonist, the observed results cannot be due to different dissociation kinetics of both ligands.[28] However, to clearly confirm an allosteric binding mode, dissociation kinetic studies would be required, which, however, cannot be performed at present due to a lack of an appropriate radiolabeled or fluorescent-labeled ligand.[23, 28]

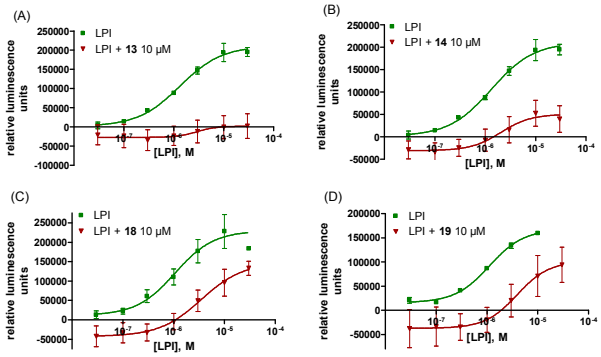

Figure 5. Concentration-response curve of LPI in β-arrestin assays in the absence and presence (10 µM) of (A) **13** (LPI EC_{50} 1.30 ± 0.18 µM, LPI + **13** EC_{50} 17.7 ± 12.3 µM), (B) **14** (LPI EC_{50} 1.12 ± 0.06 µM, LPI + **14** EC_{50} 5.10 ± 2.72 µM), (C) **18** (LPI EC_{50} 1.29 ± 0.17 µM, LPI + **18** EC_{50} 2.40 ± 0.18 µM) and (D) **19** (LPI EC_{50} 1.16 ± 0.07 µM, LPI + **19** EC_{50} 3.07 ± 0.38 µM) at CHO cells stably expressing the human GPR55. Data represent means of three independent experiments performed in duplicates.

Compound **43** is the only compound of the present series displaying significant agonistic activity at GPR55. Compared to LPI, **43** displayed similar efficacy, and can therefore be characterized as a full agonist (Figure 6). Compound **43** is an imidazo[2,1-*b*]thiazepine substituted with a bulky *p*-chlorobenzyloxybenzylidene residue. Our results showed that imidazo[2,1-*b*]thiazines and imidazo[2,1-*b*]thiazepines containing large, bulky substituents, are generally not well tolerated by GPR55. (Formal) moving of the chlorine atom of **43** from the *para*- to the *meta*- (**44**) or *ortho*-position (**45**) abolished affinity of the respective compounds for GPR55. These results indicate steep SARs of the investigated scaffolds regarding their interaction with GPR55. Comparable results had been reported for the diphenylpyrazole derivatives 1-(2,4-dichlorophenyl)-5-(4-iodophenyl)-4-methyl-*N*-1-**piperidinyl**-1*H*-pyrazole-3-carboxamide (AM251) and 1-(2,4-dichlorophenyl)-5-(4-iodophenyl)-4-methyl-*N*-4-**morpholinyl**-1*H*-pyrazole-3-carboxamide (AM281, **6**).[16] The displacement of the piperidinyl residue in AM251 by a morpholinyl residue in **6** was shown to lead to a more than 20-fold reduction in activity at GPR55 (AM251 EC_{50} 0.63 µM, **6** EC_{50} 13.6 µM, calcium mobilization assay).[16]

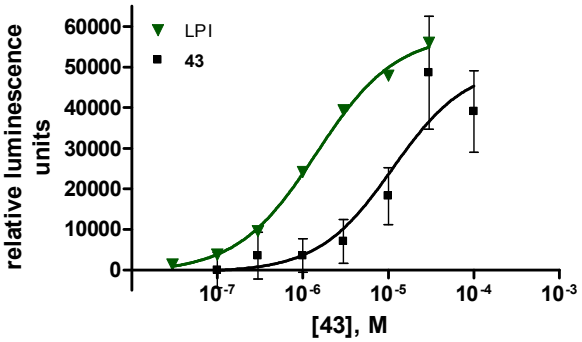

Figure 6. Concentration-dependent β-arrestin recruitment to GPR55 induced by **43** (filled squares) (EC_{50} 10.7 ± 0.3 μM). **43** exhibited comparable efficacy as LPI (green triangles) and was therefore characterized as a full agonist. Data are expressed as means ± SEM of three separate experiments performed in duplicates.

Functional properties of bicyclic imidazol-4-one derivatives at cannabinoid receptors

In order to determine the intrinsic activity of the present series at CB receptors, we investigated the compounds with the highest affinity as determined in radioligand binding studies additionally for their function (agonistic, antagonistic, inverse agonistic activity). Therefore, [^{35}S]GTPγS binding assays were performed at human recombinant and at rat brain CB_1 receptors. GDP-GTP exchange is an early event in the signal transduction mechanism of a GPCR. Measuring the binding of [^{35}S]GTPγS – a radiolabeled nonhydrolyzable analogue of GTP – provides direct quantitative information on the interaction between the receptor and the associated G protein. Binding of an agonist to the GPCR will increase binding of the guanine nucleotide, while a neutral antagonist will have no effect, and an inverse agonist will decrease [^{35}S]GTPγS binding to the G protein. The compounds were tested at a concentration of 10 μM, and the determined effects were compared to those elicited by the full agonist **7** (10 μM) and the inverse agonist **6** (10 μM).
As expected, **7** induced an increase in [^{35}S]GTPγS binding from a basal level of 100 % to to 161% in membranes prepared from human embryonic kidney (HEK293) cells expressing the human CB_1 receptor, and to 132% at CB_1 receptors natively expressed in rat brain cortical membranes. The effects of the investigated compounds were normalized to the effect evoked by **7** (see Figure 7 and Table 2 in Supplementary Information).

Antagonist **6**, previously described as an inverse agonist,[48] led to a large reduction of GTPγS binding from 0 to -80 % at human CB_1 receptors expressed in HEK293 cells. However, compound **6** had only little effect on [^{35}S]GTPγS binding to natively expressed CB_1 receptors in rat brain cortex. The discrepancy in the efficacy of the inverse agonist **6** at native (rat) CB_1 receptors compared to (human) CB_1 receptors expressed in HEK293 cells is likely due to the higher density of CB_1 receptors in the overexpressing recombinant cell system as compared to native brain tissue. Similar effects had been observed before e.g. for the antagonist/inverse agonist **5**.[49, 50]

None of the investigated compounds led to an increase in GTPγS binding at rat brain CB_1 receptors, thus showing that they were all antagonists (see Supplementary Information, Table S4).

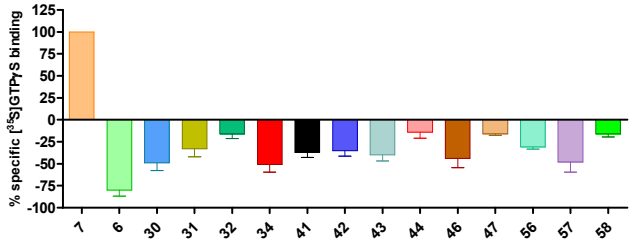

Figure 7. [^{35}S]GTPγS binding assay at human CB_1 cannabinoid receptors expressed in human embryonic kidney (HEK293) cells. All compounds were tested at a concentration of 10 μM. Obtained data were normalized with respect to the maximal effect of **7** (10 μM, set at 100 %). Data are expressed as means ± SEM of at least three separate experiments performed in triplicate.

In HEK293 cells, which were stably transfected with the human CB_1 receptor, the selected imidazol-4-one derivatives induced a decrease in basal [^{35}S]GTPγS binding by 14% to 51%, indicating inverse agonistic activity of the compounds in a test system with receptor overexpression. Compounds **30**, **34**, **43**, **46** and **57** displayed the greatest negative intrinsic activity (up to approximatly -50%). The investigated compounds showed in most cases a good correlation between their affinity and the effects observed in GTPγS binding studies, with only few exceptions. The *p*-fluorobenzyloxy-benzylidene-substituted imidazo[2,1-*b*]thiazepine derivative (**47**) showed high CB_1 receptor affinity, but showed only a low degree of inverse agonistic activity when compared to the unsubstituted benzyloxybenzylidene analogue **42**. The *m*-chlorobenzyloxy-benzylidene derivative (**44**) displayed similarly low intrinsic activity as **47**. Compound **57**, a 5,5-diphenylimidazo[2,1-*b*]thiazepine, exhibited an approximately 5-fold decreased affinity to the rat CB_1 receptor compared to its 6,6-diphenylimidazo[2,1-*b*]thiazepine analogue **58**, but **57** had a greater negative intrinsic activity (-48 % (**57**) compared to -16 % (**58**)), indicating that the position of the annelated sulfur-containing heterocycle may have an impact on the efficacy of the compounds. Further GTPγS binding studies showed that compound **43** displayed inverse agonistic activity also at the human recombinant CB_2 receptor subtype where it decreased basal [^{35}S]GTPγS binding (see Supplementary Information, Table S4).

Finally, the most potent CB_1 (**34**, **43**, **47**, **58**) and CB_2 antagonists (**31**, **34**, **42**, **45**, **46**, **47**) of the present series were additionally investigated for potential effects on forskolin-induced cAMP accumulation in CHO-K1 cells stably expressing either human CB_1 or CB_2 receptors (see Supplementary Information, Figure S1 and S2). In contrast to the agonist **7**, none of the test compounds showed any effect at a high concentration of 10 μM indicating that they are receptor antagonists, and thus confirming the results obtained in GTPγS binding studies.

Conclusions

Imidazo[2,1-*b*]thiazole (**51-54**), imidazo[2,1-*b*]thiazine (**10-39**, **55-56**), and imidazo[2,1-*b*]thiazepine derivatives (**57-58**, **40-50**) were discovered as new scaffolds for the development of antagonists for the orphan GPCRs GPR18 and GPR55, and for the CB receptor subtypes CB_1 and CB_2. Introduction of a benzoyloxybenzylidene residue (**36**, GPR18 IC_{50} 6.35 μM, GPR55 and CB_1 K_i >10 μM, CB_2 K_i ~ 10 μM) or a *p*-chlorobenzyloxybenzylidene residue (**32**, GPR18 IC_{50} 0.279 μM, GPR55 and CB_1 K_i >10 μM, CB_2 K_i 4.03 μM) into an imidazo[2,1-*b*]thiazine scaffold led to GPR18-selective antagonists. Compound **32** exhibited the highest inhibitory potency

of all investigated compounds at GPR18 combined with >>36-fold selectivity over CB_1 and 14-fold selectivity over CB_2 receptors. The compound did not interact with GPR55. To our knowledge, GPR18 antagonist **32** represents the first selective antagonist for this poorly investigated orphan receptor, which appears to have considerable potential as a novel drug target.

Contrary to CB_1, CB_2 and GPR18, our results indicate that GPR55 preferentially interacts with imidazo[2,1-*b*]thiazine derivatives possessing benzylidene residues without bulky substituents. The identified ligands of this subgroup, such as **18** and **19**, displayed antagonistic activity at GPR55 (**18** IC_{50} 3.15 µM, **19** IC_{50} 3.46 µM) and in general no affinity to CB receptors. The identified GPR55 antagonists did also not interact with GPR18. Thus, these new GPR55 antagonists represent suitable lead structures for the development of more potent, selective GPR55 antagonists. In addition to antagonists, we also identified one GPR55 receptor agonist (**43**, EC_{50} 10.7 µM). Interestingly, **43** also displayed high affinity for CB receptors, but showed contrary intrinsic activity at CB receptors where it acted as an antagonist / inverse agonist. This phenomenon – reverse intrinsic activity at GPR55 versus CB receptors – had previously been reported for other CB receptor ligands, including **1**, **5** and **7**, and led to the designation of GPR55 as an 'anti-cannabinoid receptor'.[28, 51] Compound **43** was the most potent ligand at CB_1 receptors and exhibited 17-fold selectivity over CB_2 receptors (K_i CB_1 0.25 µM; CB_2 K_i 4.15 µM). The compound showed only a very weak inhibitory effect at the GPR18.

In addition to selective antagonists for either of the investigated subtypes, compounds were identified which block GPR18 as well as CB_1 and CB_2 receptors at a similar concentration while not interacting with GPR55. The best triply active antagonist was **34** (GPR18 IC_{50} 2.55 µM, CB_1 K_i 2.09 µM, CB_2, K_i 0.95 µM), which may become a useful research tool to study effects of the blockade of all three CB(-like) receptors.

This very first extensive SAR study of a series of 49 ligands investigated at all four CB and CB-like receptors reveals structural requirements for the development of potent and selective GPR18 and GPR55 antagonists. Selective GPR18 and GPR55 antagonists are crucial tools to pharmacologically characterize these orphan GPCRs, to explore their (patho-)physiological role and their potential as future drug targets.

Experimental Section

Syntheses

Melting points were measured in open capillaries on a Mel-Temp. II apparatus (LD Inc., USA) and were not corrected. The purity of the synthesized compounds was confirmed by TLC performed on Merck silica gel 60 GF_{254} aluminium sheets (Merck, Darmstadt, Germany), using the following developing system: $CHCl_3$: AcOEt (1/1, v/v). Spots were detected by their absorption under UV light (λ = 254 nm). Column chromatography was performed on Merck silica gel 60 (70-230 mesh) using CH_2Cl_2 : AcOEt; 1/1 (v/v) as an eluent. Infrared spectra were measured with an FT IR 410 spectrometer (Jasco) in KBr pellets. ^{1}H-NMR spectra were obtained on a Varian Mercury spectrometer (Varian Inc., Palo Alto, CA, USA) in DMSO-d_6 or $CDCl_3$ operating at 300 MHz. Chemical shifts are reported in δ values (ppm) relative to undeuterated solvent signals. The *J* values are expressed in Hertz (Hz). Signal multiplicities are represented by the following abbreviations: s (singlet), d (doublet), dd (double dublet), t (triplet), def.t. (deformated triplet), m (multiplet). ^{13}H-NMR spectra were acquired on a Varian Mercury spectrometer (Varian Inc., Palo Alto, CA, USA) in $CDCl_3$, operating at 75 MHz. Mass spectrometry analyses: samples were prepared in a mixture of acetonitrile : water (50/50, v/v). The LC/MS system consisted of a Waters Acquity UPLC, coupled to a Waters TQD mass spectrometer (electrospray ionization mode ESI-tandem quadrupole). All analyses were carried out using an Acquity UPLC BEH C18, 100 x 2.1 mm reversed-phase column. A flow rate of 0.3 mL/min and a gradient of 5-100 % B over 10 min was used. Eluent A: water containing 0.1% HCO_2H; eluent B: acetonitrile containing 0.1% HCO_2H. Nitrogen was used as both, nebulizing and drying gas. LC/MS data were obtained by scanning the first quadrupole in 0.5 s in a mass range from 50 to 1000 m/z; 10 scans were summed up to produce the final spectrum. Mass chromatograms of specific ions were recorded by tuning the first quadrupole on a targeted m/z value known as single ion recording experiment. LC/MS/MS data were obtained upon low energy collision induced dissociation (CID) conditions. The first quadrupole was fixed to the m/z value corresponding to the precursor ion to be dissociated, the collision cell (q) was filled with argon as collision gas and the last quadrupole was scanned within 0.5 s from 100 to 500 m/z; 10 scans were summed up to produce the final daughter ion mass spectra. Elemental analyses for C, H, N and S were carried out by a micro method using the elemental Vario-EL III Elemental Analyser (Hanau, Germany) and were found within ± 0.4% of the theoretical values. All tested compounds possessed a purity of not less than 95%.

Compounds **12**, **13**, **23**, **24**, **29**[1]; **11**, **21**[29, 35]; **10**, **20**, **22**[32]; **57**, **58**[36]; **14**, **25, 27**, **28**, **30**, **38**, **39**[34]; **56**[37, 38]; **52**, **54**[30]; **51**, **55**[31]; and **40**, **41**, **43**, **46**, **48, 49**, **50**[33] were prepared as described.

Preparation of imidazo[2,1-*b*][1,3]thiazinones 15-19, **31-37 and imidazo[2,1-*b*][1,3]thiazepinones 42**, **44**, **45**, **47**

The new compounds **15-19**, **31-37**, **42**, **44**, **45** and **47** were prepared in analogy to described procedures.[29, 32] The general procedure was as follows:

To a stirred suspension of the appropriate (*Z*)-5-arylidene-2-thiohydantoin (0.01 mol), K_2CO_3 (0.029 mol) and benzyltriethylammonium chloride (0.001 mol) in 50 ml acetone, a solution of 1,3-dibromopropane (0.01 mol), or 1,4-dibromobutane (0.012 mol), respectively, in 10 ml acetone was added dropwise. The suspension was stirred for 48. Then the precipitate was filtered off, washed with water, then with 1% aq. NaOH, followed by 1% aq. HCl solutions (50 mL each). The remaining solid was suspended in chloroform (100 ml), stirred for 0.5 h, and the suspension was filtered. The solid (mp > 220°C) was discarded. The chloroform filtrate was evaporated to dryness, the residue was dissolved in chloroform and washed with water, followed by 1% aq. NaOH solution (50 mL each), and then evaporated to dryness. The obtained solids or oily residues, were purified by means of column chromatography.

Analytical data

(*Z*)-2-(2,4-Dichlorobenzylidene)-6,7-dihydro-2*H*-imidazo[2,1-*b*]-[1,3]thiazin-3(5*H*)-one (15) Product **15** was purified by crystallization; yellow powder, m.p. 225-228°C (acetonitrile); yield 14.47 %; ^{1}H-NMR (300 MHz; $CDCl_3$) δ: 2.24-2.32 (m, 2H, $SCH_2C\underline{H}_2$), 3.15 (def. t, *J*=5.77 Hz, 2H, SCH_2), 3.61 (t, *J*=5.90 Hz, 2H, NCH_2), 7.25-7.29 (m, 1H, Ar H-5'), 7.31 (s, 1H, ArCH=), 7.41 (d, *J*=2.05 Hz, 1H, Ar H-3'), 8.75 (d, *J*=7.84 Hz, 1H, Ar H-6'); ^{13}C-NMR (75 MHz; $CDCl_3$) δ: 22.80 (CH_2); 26.20 (SCH_2); 39.86 (NCH_2); 117.43 (ArCH=); 127.43; 129.43; 130.74; 133.77; 135.62;

136.31; 138.50(ArCH=C); 161.99 (C=O); 168.44 (C=N); IR ν: 1707(C=O), 1629(ArCH=), 1578(C=N), 1481, 1462, 1362, 1282, 1261, 1165, 1117; R_f = 0.61; t_R = 7.81; purity 98.46%; MS calcd for $[M+H]^+$: $C_{13}H_{10}N_2OSCl_2$ m/z: 313.20, found 313.21; Anal. Calcd: C 49.85, H 3.22, N 8.95, S 10.24; Found: C, 50.19, H 3.57, N 9.12, S 10.77.

(*Z*)-2-(2,6-Dichlorobenzylidene)-6,7-dihydro-2*H*-imidazo[2,1-*b*][1,3]thiazin-3(5*H*)-one (16) Product **16** was purified by crystallization; cream yellow powder, m.p. 228-231°C (acetonitrile); yield 41.9 %; ^{1}H-NMR (300 MHz; $CDCl_3$) δ: 2.23-2.31 (m, 2H, SCH_2CH_2), 3.11 (def. t, *J*=5.64 Hz, 2H, SCH_2), 3.74 (t, *J*=5.89 Hz, 2H, NCH_2), 7.00 (s, 1H, ArCH=), 7.16-7.25 (m, 1H, Ar H-4'), 7.32 (d, *J*=8.46 Hz, 2H, Ar H-3', Ar H-5'); ^{13}C-NMR (75 MHz; $CDCl_3$) δ: 23.00 (CH_2); 26.11 (SCH_2); 39.97 (NCH_2); 119.16 (ArCH=); 128.17; 129.85; 132.00; 136.00; 141.00 (ArCH=C); 163.00 (C=O); 169.00 (C=N); IR ν: 1719(C=O), 1644(ArCH=), 1554(C=N), 1494, 1471, 1425, 1392, 1329, 1245, 1164, 1121, 1093, 773; R_f = 0.58; t_R = 5.90; purity 99.56%; MS calcd for $[M+H]^+$: $C_{13}H_{10}N_2OSCl_2$ m/z: 313.20, found 313.14; Anal. Calcd: C 49.85, H 3.22, N 8.95, S 10.24; Found: C, 50.03, H 3.42, N 8.91, S 10.71.

(*Z*)-2-(2-Fluorobenzylidene)-6,7-dihydro-2*H*-imidazo[2,1-*b*][1,3]thiazin-3(5*H*)-one (17) Product **17** was purified by crystallization; yellow powder, m.p. 199-202°C (acetonitrile); yield 12.7 %; ^{1}H-NMR (300 MHz; $CDCl_3$) δ: 2.27-2.32 (m, 2H, SCH_2CH_2), 3.16 (def. t, *J*=5.64 Hz, 2H, SCH_2), 3.75 (t, *J*=5.77 Hz, 2H, NCH_2), 7.05 (dt, J_1=9.29 Hz, J_2=1.16 Hz, 1H, Ar H-3'), 7.17 – 7.22 (m, 1H, Ar H-4'); 7.27 (s, 1H, ArCH=), 7.29 – 7.36 (m, 1H, Ar H-5'); 8.74 (dt, J_1=7.69 Hz, J_2=1.79 Hz, 1H, Ar H-6'), ^{13}C-NMR (75 MHz; $CDCl_3$) δ: 22.87 (CH_2); 26.16 (SCH_2); 39.85 (NCH_2); 114.72 (ArCH=); 115.07; 122.49; 124.45; 131.41; 132.61; 138.16; 161.00 (ArCH=C); 163.40 (C=O); 168.60 (C=N); IR ν: 1704(C=O), 1632(ArCH=), 1552(C=N), 1489, 1455, 1292, 1230, 1166, 1128, 762; R_f = 0.62; t_R = 6.09; purity 99.44%; MS calcd for $[M+H]^+$: $C_{13}H_{11}N_2OSF$ m/z: 262.30, found 263.28.

(*Z*)-2-(2,3-Difluorobenzylidene)-6,7-dihydro-2*H*-imidazo[2,1-*b*][1,3]thiazin-3(5*H*)-one (18) Product **18** was purified by crystallization; yellow powder, m.p. 227-230°C (acetonitrile); yield 17.86 %; ^{1}H-NMR (300 MHz; $CDCl_3$) δ: 2.25-2.33 (m, 2H, SCH_2CH_2), 3.17 (def. t, *J*=5.76 Hz, 2H, SCH_2), 3.76 (t, *J*=5.90 Hz, 2H, NCH_2), 7.08-7.16 (m, 2H, Ar H-4', Ar H-5'), 7.20 (s, 1H, ArCH=), 8.47 – 8.53 (m, 1H, Ar H-6'); 8.74 (dt, J_1=7.69 Hz, J_2=1.79 Hz, 1H, Ar H-6'), ^{13}C-NMR (75 MHz; $CDCl_3$) δ: 22.82 (CH_2); 26.18 (SCH_2); 39.87 (NCH_2); 113.12; 117.90 (ArCH=); 124.15; 124.53; 127.33; 139.00; 147.92; 151.31(ArCH=C); 162.08 (C=O); 168.46 (C=N); R_f = 0.64; t_R = 6.42; purity 98.18%; MS calcd for $[M+H]^+$: $C_{13}H_{10}N_2OSF_2$ m/z: 280.30, found 281.23.

(*Z*)-2-(2,4-Difluorobenzylidene)-6,7-dihydro-2*H*-imidazo[2,1-*b*][1,3]thiazin-3(5*H*)-one (19) Product (**19**) was purified by column chromatography and crystallization; yellow powder, m.p. 211-214°C (acetonitrile); yield 11.9%; ^{1}H-NMR (300 MHz; $CDCl_3$) δ: 2.24-2.32 (m, 2H, SCH_2CH_2), 3.16 (def. t, *J*=5.64 Hz, 2H, SCH_2), 3.75 (t, *J*=5.90 Hz, 2H, NCH_2), 6.77 – 6.85 (m, 1H, Ar H-5'); 6.90 – 6.97 (m, 1H, Ar H-3'), 7.17 (s, 1H, ArCH=), 8.80 (dq, J_1=6.92 Hz, J_2=1.92 Hz, 1H, Ar H-6'), ^{13}C-NMR (75 MHz; $CDCl_3$) δ: 22.87 (CH_2); 26.15 (SCH_2); 39.85 (NCH_2); 103.37 (ArCH=); 111.85; 118.87; 133.84; 134.00; 137.93; 160.23; 161.83(ArCH=C); 163.64 (C=O); 168.59 (C=N); R_f = 0.68; t_R = 6.46; purity 99.36b%; MS calcd for $[M+H]^+$: $C_{13}H_{10}N_2OSF$ m/z: 280.30, found 281.23.

(*Z*)-2-(2,4-Dimethoxybenzylidene)-6,7-dihydro-2*H*-imidazo[2,1-*b*][1,3]thiazin-3(5*H*)-one (26) Product **26** was purified by crystallization; light yellow powder, m.p. 199-202°C (acetonitrile); yield 18.6 %; ^{1}H-NMR (300 MHz; $CDCl_3$) δ: 2.23-2.30 (m, 2H, SCH_2CH_2), 3.13 (def. t, *J*=5.64 Hz, 2H, SCH_2), 3.73 (t, *J*=5.90 Hz, 2H, NCH_2), 3.86 (s, 3H, OCH_3), 3.87 (s, 3H, OCH_3), 6.91 (dd, J_1=8.20 Hz, J_2=1.54 Hz, 1H, Ar H-4'), 7.09 (t, *J*=8.33 Hz,1H, Ar H-5'), 7.43 (s, 1H, ArCH=), 8.30 (dd, J_1=8.08 Hz, J_2=1.41 Hz, 1H, Ar H-6'); ^{13}C-NMR (75 MHz; $CDCl_3$) δ: 22.92 (CH_2); 26.14 (SCH_2); 39.83 (NCH_2); 55.82 (OCH_3); 61.75 (OCH_3); 113.97 (ArCH=); 118.19; 124.15; 124.19; 128.40; 137.75; 149.28; 152.51 (ArCH=C); 159.98 (C=O); 168.87 (C=N); IR ν: 1708(C=O), 1625(ArCH=), 1573(C=N), 1493, 1469, 1425, 1271, 1237, 1188, 1168, 1121, 1063, 997, 739; R_f = 0.61; t_R = 5.68; purity 95.09%; MS calcd for $[M+H]^+$: $C_{15}H_{16}N_2O_3S$ m/z: 304.36, found 305.23; Anal. Calcd: C 59.16, H 5.30, N 9.21, S 10.53; Found: C 58.72, H 5.24, N 9.20, S 10.36.

(*Z*)-2-(3-(Benzyloxy)benzylidene)-6,7-dihydro-2*H*-imidazo[2,1-*b*][1,3]thiazin-3(5*H*)-one (31) Product **31** was obtained after purification by column chromatography; yellow powder, m.p. 189-191°C (dioxane); yield 15 %; ^{1}H-NMR (300 MHz; DMSO-d_6) δ: 2.15-2.16 (m, 2H, SCH_2CH_2), 3.22 (def. t, *J*=5.47 Hz, 2H, SCH_2), 3.61 (t, *J*=5.64 Hz, 2H, NCH_2), 5.11 (s, 2H, CH_2O), 6.77 (s, 1H, ArCH=), 7.02 (dd, *J*=8.20 Hz, *J*=1.80 Hz, 1H, Ar H-4'), 7.29-7.41 (m, 4H, Ar H-5', Ar H-3'', H-4'', H-5''), 7.46 (dd, *J*=7.18 Hz, *J*=1.60 Hz, 2H, Ar H-2'', H-6''), 7.67 (d, *J*=7.60 Hz, 1H, Ar H-6'), 7.86 (d, *J*=1.53 Hz, 1H, Ar H-2'); ^{13}C-NMR (75 MHz; $CDCl_3$) δ: 22.92 (CH_2); 26.11 (SCH_2); 39.85 (NCH_2); 70.05 (CH_2O); 117.10; 117.21; 124.06; 125.08; 127.74; 127.99; 128.58; 129.56; 135.50; 136.89; 137.52; 158.81 (ArCH=C); 160.02 (C=O); 168.96 (C=N); IR ν: 1709(C=O), 1637(ArCH=), 1569(C=N), 1489, 1446, 1290, 1259, 1160, 1041, 747; R_f = 0.49; t_R = 7.46; purity 98.22%; MS calcd for $[M+H]^+$: $C_{20}H_{18}N_2O_2SC$ m/z: 350.42, found 351.2; Anal. Calcd: C 68.55, H 5.18, N 7.99, S 9.15; Found: C, 68.56, H 5.02, N 7.81, S 8.73.

(*Z*)-2-(3-(4-Chlorobenzyloxy)benzylidene)-6,7-dihydro-2*H*-imidazo[2,1-*b*][1,3]thiazin-3(5*H*)-one (32) Product **32** was obtained by column chromatography; yellow powder, mp. 189-191°C; yield 12 %; ^{1}H-NMR (300 MHz; DMSO-d_6) δ: 2.12-2.16 (m, 2H, SCH_2CH_2), 3.21 (def. t, *J*=5.51 Hz, 2H, SCH_2), 3.60 (t, *J*=5.79 Hz, 2H, NCH_2), 5.10 (s, 2H, CH_2O), 6.77 (s, 1H, ArCH=), 7.00 (dd, *J*=8.46 Hz, *J*=2.05 Hz, 1H, Ar H-4'), 7.32 (def.t, *J*=8.20 Hz, 1H, Ar H-5'), 7.41-7.50 (m, 4H, Ar H-5'', H-3'', Ar H-2'', H-6''), 7.67 (d, *J*=7.95 Hz, 1H, Ar H-6'), 7.85 (d, *J*=2.31 Hz, 1H, Ar H-2'); ^{13}C-NMR (75 MHz; $CDCl_3$) δ: 22.94 (CH_2); 26.12 (SCH_2); 39.85 (NCH_2); 69.22 (CH_2O); 116.84; 117.28; 123.87; 125.29; 128.73; 129.05; 129.58; 133.72; 135.44; 135.57; 137.67; 158.52 (ArCH=C); 160.04 (C=O); 168.97 (C=N); IR ν: 1703(C=O), 1636(ArCH=), 1578(C=N), 1494, 1473, 1358, 1231, 1178, 1033, 797; R_f = 0.49; t_R = 8.05; purity 97.07%; MS calcd for $[M+H]^+$: $C_{20}H_{17}N_2O_2ClS$ m/z: 384.9, found 385.1; CC (CH_2Cl_2 : AcOEt 1 : 1); Anal. Calcd: C 62.41, H 4.45, N 7.28, S 8.33; Found: C, 62.22, H 4.58, N 7.10, S 8.51.

(*Z*)-2-(3-(2-Chlorobenzyloxy)benzylidene)-6,7-dihydro-2*H*-imidazo[2,1-*b*][1,3]thiazin-3(5*H*)-one (33) Product **33** was purified by crystallization; yellow powder, mp. 171-173°C (twice crystallization acetonitrile); yield 14.38 %; ^{1}H-NMR (300 MHz; $CDCl_3$) δ: 2.23-2.30 (m, 2H, SCH_2CH_2), 3.13 (def. t, *J*=5.64 Hz, 2H, SCH_2), 3.73 (t, *J*=5.77 Hz, 2H, NCH_2), 5.22 (s, 2H, CH_2O), 6.92 (s, 1H, ArCH=), 6.98 (dd, *J*=8.25 Hz, *J*=0.77 Hz, 1H, Ar H-4'), 7.24-7.37(m, 3H, Ar H-3'', Ar H-4'', H-6''), 7.41 (m, 1H, Ar H-5'), 7.56-7.59 (m, 1H, Ar H-6''); 7.64 (d, *J*=7.69 Hz, 1H, Ar H-6'), 7.86 (t,

J=8.05 Hz, 1H, Ar H-2'); ^{13}C-NMR (75 MHz; $CDCl_3$) δ: 22.93 (CH_2); 26.12 (SCH_2); 39.86 (NCH_2); 67.21 (CH_2O); 116.97; 117.36; 123.92; 125.22; 126.94; 128.94; 128.99; 129.41; 129.63; 132.71; 134.62; 135.58; 137.61; 158.52 (ArCH=C); 160.09 (C=O); 168.96 (C=N); IR ν: 1714(C=O), 1632(ArCH=), 1578(C=N), 1484, 1437, 1360, 1288, 1263, 1155, 1017, 759; R_f = 0.62; t_R = 8.09; purity 99.13%; MS calcd for $[M+H]^+$: $C_{20}H_{17}N_2O_2ClS$ m/z: 384.88, found 385.27; Anal. Calcd: C 62.41, H 4.45, N 7.28, S 8.33; Found: C, 62.36, H 4.98, N 7.37, S 8.40.

(*Z*)-2-(3-(2,4-Dichlorobenzyloxy)benzylidene)-6,7-dihydro-2*H*-imidazo[2,1-*b*][1,3]thiazin-3(5*H*)-one (34) Product **34** was purified by column chromatography; yellow powder, mp. 160-162°C; yield 13 %; ^{1}H-NMR (300 MHz) δ: 2.15 (def.t, *J*=2.43 Hz, 2H, SCH_2CH_2), 3.21 (def. t, *J*=5.51 Hz, 2H, SCH_2), 3.60 (t, *J*=5.64 Hz, 2H, NCH_2), 5.15 (s, 2H, CH_2O), 6.78 (s, 1H, ArCH=), 7.03 (dd, *J*=7.71 Hz, *J*=2.30 Hz, 1H, Ar H-4'), 7.34 (t, *J*=8.08 Hz, 1H, Ar H-5'), 7.43 (d, *J*=2.05 Hz, 1H, Ar H-5''), 7.47 (d, *J*=2.31 Hz, 1H, Ar H-3''), 7.58-7.69 (m, 2H, Ar H-6'', H-6'), 7.88 (s, 1H, Ar H-2'); ^{13}C-NMR (75 MHz; $CDCl_3$) δ: 22.92 (CH_2); 26.12 (SCH_2); 39.85 (NCH_2); 66.66 (CH_2O); 116.98; 117.13; 123.68; 125.42; 127.27; 129.22; 129.65; 129.76; 133.27; 133.33; 134.05; 135.66; 137.72; 158.26(ArCH=C); 160.20 (C=O); 168.93 (C=N); IR ν: 1709(C=O), 1634(ArCH=), 1572(C=N), 1486, 1443, 1294, 1258, 1161, 1045, 907, 779; R_f = 0.51; t_R = 8.81; purity 98.11%; MS calcd for $[M+H]^+$: $C_{20}H_{18}N_2O_2Cl_2S$ m/z: 419.3, found 419.1; CC (CH_2Cl_2 : AcOEt 1 : 1); Anal. Calcd: C 57.28, H 3.84, N 6.68, S 7.65; Found: C, 57.03, H 4.18, N 6.64, S 7.73.

(*Z*)-2-(3-(3,4-Dichlorobenzyloxy)benzylidene)-6,7-dihydro-2*H*-imidazo[2,1-*b*][1,3]thiazin-3(5*H*)-one (35) Product **35** was purified by crystallization; yellow powder, mp. 188-191°C (acetonitrile); yield 14.94 %; ^{1}H-NMR (300 MHz; $CDCl_3$) δ: 2.23-2.31 (m, 2H, SCH_2CH_2), 3.15 (def. t, *J*=5.64 Hz, 2H, SCH_2), 3.73 (t, *J*=5.90 Hz, 2H, NCH_2), 5.06 (s, 2H, CH_2O), 6.90 (s, 1H, ArCH=), 6.94 (dd, *J*=7.87 Hz, *J*=1.03 Hz, 1H, Ar H-4'), 7.26-7.32 (m, 2H, Ar H-2'', Ar H-5''), 7.45 (d, *J*=8.20 Hz, 1H, Ar H-6''), 7.53-7.57 (m, 2H, Ar H-5', H-6'), 7.89-7.91 (m, 1H, Ar H-2'); ^{13}C-NMR (75 MHz; $CDCl_3$) δ: 22.92 (CH_2); 26.15 (SCH_2); 39.86 (NCH_2); 68.53 (CH_2O); 116.68 (ArCH=); 117.31; 123.76; 125.51; 126.81; 129.38; 129.65; 130.53; 131.89; 132.68; 135.59; 137.26; 137.54; 158.29 (ArCH=C); 160.23 (C=O); 168.88 (C=N); IR ν: 1704(C=O), 1636(ArCH=), 1576(C=N), 1488, 1465, 1357, 1230, 1180, 1163, 1040, 903, 795; R_f = 0.63; t_R = 8.65; purity 99.05%; MS calcd for $[M+H]^+$: $C_{20}H_{16}N_2O_2Cl_2S$ m/z: 419.33, found 419.24; Anal. Calcd: C 57.28, H 3.85, N 6.68, S 7.65; Found: C, 57.07, H 4.11, N 6.73, S 7.58.

(*Z*)-4-((3-Oxo-6,7-dihydro-3*H*-imidazo[2,1-*b*][1,3]thiazin-2(5*H*)-ylidene)metyl)phenyl benzoate (36) Product **36** was purified by column chromatography; yellow powder, mp. 198-200°C; yield 22 %; ^{1}H-NMR (300 MHz; DMSO-d_6) δ: 2.18-2.22 (m, 2H, SCH_2CH_2), 3.25 (def. t, *J*=5.50 Hz, 2H, SCH_2), 3.66 (t, *J*=5.77 Hz, 2H, NCH_2), 6.91 (s, 1H, ArCH=), 7.39 (dd, *J*=8.80 Hz, *J*=1.93 Hz, 2H, Ar H-3', H-5'), 7.63 (t, *J*=7.56 Hz, 2H, Ar H-3'', H-5''), 7.79 (t, *J*=6.05 Hz, 1H, Ar H-4''), 8.16 (dd, *J*=6.88 Hz, *J*=1.65 Hz, 2H, Ar H-2'', H-6''), 8.27 (dd, *J*=8.80 Hz, *J*=2.48 Hz, Ar H-2', H-6'); ^{13}C-NMR (75 MHz; $CDCl_3$) δ: 22.86 (CH_2); 26.15 (SCH_2); 39.87 (NCH_2); 122.02; 123.07; 128.61; 129.93; 130.22; 132.04; 133.20; 133.72; 137.19; 151.97 (ArCH=C); 160.25 (C=O); 164.84 (C=O); 168.88 (C=N); IR ν: 1736(COO), 1713(C=O), 1634(ArCH=), 1593(C=N), 1486, 1469, 1248, 1200, 1170, 1066, 1024, 899, 712; R_f = 0.55; t_R = 7.25; purity 99.25%; MS calcd for $[M+H]^+$: $C_{20}H_{16}N_2O_3S$ m/z: 364.4, found 365.2; CC (CH_2Cl_2 : AcOEt 1 : 1); Anal. Calcd: C 65.91, H 4.43, N 7.69, S 8.80; Found: C, 65.61, H 4.68, N 7.45, S 8.49.

(*Z*)-4-((3-Oxo-6,7-dihydro-3*H*-imidazo[2,1-*b*][1,3]thiazin-2(5*H*)-ylidene)metyl)phenyl 4-chloro-benzoate (37) Product **37** was purified by column chromatography; yellow powder, mp. 212-214°C; yield 27 %; ^{1}H-NMR (300 MHz; DMSO-d_6) δ: 2.19-2.21 (m, 2H, SCH_2CH_2), 3.22-3.30 (m, 2H, SCH_2), 3.66 (t, *J*=5.64 Hz, 2H, NCH_2), 6.90 (s, 1H, ArCH=), 7.39 (d, *J*=8.80 Hz, *J*=1.92 Hz, 2H, Ar H-3', H-5'), 7.70 (d, *J*=8.50 Hz, *J*=1.92 Hz, 2H, Ar H-3'', H-5''), 8.16 (d, *J*=8.52 Hz, *J*=1.92 Hz, 2H, Ar H-2'', H-6''), 8.26 (d, *J*=8.80 Hz, *J*=1.92 Hz, 2H, Ar H-2', H-6'); ^{13}C-NMR (75 MHz; $CDCl_3$) δ: 22.86 (CH_2); 26.15 (SCH_2); 39.86 (NCH_2); 121.91; 122.96; 127.78; 128.98; 131.58; 132.16; 133.20; 137.17; 140.26; 151.72 (ArCH=C); 160.39 (C=O); 163.98 (C=O); 168.81 (C=N); IR ν: 1741(COO), 1714(C=O), 1635(ArCH=), 1591(C=N), 1482, 1358, 1259, 1199, 1163, 1067, 1013, 751; R_f = 0.59; t_R = 7.99; purity 98.96%; MS calcd for $[M+H]^+$: $C_{20}H_{15}N_2O_3SCl$ m/z: 398.9, found 399.2; CC (CH_2Cl_2 : AcOEt 1 : 1); Anal. Calcd: C 60.22, H 3.79, N 7.02, S 8.04; Found: C, 60.08, H 4.09, N 6.93, S 8.49.

(*Z*)-2-(3-(Benzyloxy)benzylidene)-5,6,7,8-tetrahydroimidazo[2,1-*b*][1,3]thiazepin-3(2*H*)-one (42) Product **42** was purified by column chromatography; yellow powder, mp. 139-141°C (acetonitrile, dioxane); yield 29 %; ^{1}H-NMR (300 MHz; DMSO-d_6) δ: 1.78 (t, *J*=4.74 Hz, 2H, SCH_2CH_2), 2.02 (t, *J*=3.20 Hz, 2H, NCH_2CH_2), 3.14 (def.t, *J*=5.38 Hz, 2H, SCH_2), 3.72 (def.t, *J*=5.00 Hz, 2H, NCH_2), 5.11 (s, 2H, CH_2O), 6.93 (s, 1H, ArCH=), 7.07 (dd, *J*=6.41 Hz, *J*=2.31 Hz, 1H, Ar H-4'), 7.28-7.41 (m, 4H, Ar H-5', H-3'', H-4'', H-5''), 7.47 (dd, *J*=9.48 Hz, *J*=1.41 Hz, 2H, Ar H-2'', H-6''), 7.71 (d, *J*=7.95 Hz, 1H, Ar H-2'), 7.91 (d, *J*=1.54 Hz, 1H, Ar H-6'); ^{13}C-NMR (75 MHz; $CDCl_3$) δ: 28.16 (CH_2); 31,03 (CH_2); 32.43 (SCH_2); 41.06 (NCH_2); 70.06 (CH_2O); 117.48; 117.82; 125.49; 127.38; 127.77; 127.85; 128.02; 128.58; 128.76; 129.67; 135.20; 136.79; 138.94; 158.84 (ArCH=C); 164.92 (C=O); 169.60 (C=N); IR ν: 1703(C=O), 1632(ArCH=), 1580(C=N), 1488, 1437, 1337, 1287, 1262, 1178, 1154, 1022, 787, 748, 700; R_f = 0.84; t_R = 8.03; purity 98.82%; MS calcd for $[M+H]^+$: $C_{21}H_{20}N_2O_2S$ m/z: 364.4, found 365.3; Anal. Calcd: C 69.20, H 5.53, N 7.69, S 8.80; Found: C, 69.12, H 5.66, N 7.67, S 9.14.

(*Z*)-2-(3-(3-Chlorobenzyloxy)benzylidene)-5,6,7,8-tetrahydroimidazo[2,1-*b*][1,3]thiazepin-3(2*H*)-one (44) Product **44** was purified by column chromatography; yellow powder, mp. 129-131°C; Yield 16 %; ^{1}H-NMR (300 MHz; DMSO-d_6) δ: 1.77 (def.t, 2H, SCH_2CH_2), 2.01 (def.t, 2H, NCH_2CH_2), 3.14 (def.t, *J*=5.38 Hz, 2H, SCH_2), 3.72 (t, *J*=4.87 Hz, 2H, NCH_2), 5.13 (s, 2H, CH_2O), 6.93 (s, 1H, ArCH=), 7.05 (dd, *J*=7.94 Hz, *J*=2.31 Hz, 1H, Ar H-4'), 7.32-7.45 (m, 4H, Ar H-5', Ar H-4'', H-5'', H-6''), 7.53 (s, 1H, Ar H-2''), 7.73 (d, *J*=7.95 Hz, 1H, Ar H-6'), 7.90 (d, *J*=1.54 Hz, 1H, Ar H-2'); ^{13}C-NMR (75 MHz; $CDCl_3$) δ: 28.12 (CH_2); 30.98 (CH_2); 32.46 (SCH_2); 41.09 (NCH_2); 69.17 (CH_2O); 117.22; 117,91; 125.27; 125.65; 125.78; 127.63; 127.68; 128.13; 129.73; 129.85; 134.46; 135.21; 138.90; 158.52 (ArCH=C); 165.13 (C=O); 169.46 (C=N); IR ν: 1725(C=O), 1649(ArCH=), 1579(C=N), 1488, 1372, 1235, 1161, 953, 779, 681; R_f = 0.83 ($CHCl_3$:AcOEt 1:1); t_R = 8.58; purity 98.46%; MS calcd for $[M+H]^+$: $C_{21}H_{19}N_2O_2ClS$ m/z: 398.9, found 399.2; CC (CH_2Cl_2 : AcOEt 1 : 1); Anal. Calcd: C 63.22, H 4.80, N 7.02, S 8.04; Found: C, 63.45, H 5.14, N 6.86, S 7.97.

(*Z*)-2-(3-(2-Chlorobenzyloxy)benzylidene)-5,6,7,8-tetrahydroimidazo[2,1-*b*][1,3]thiazepin-3(2*H*)-one (45) Product **45** was purified by column chromatography; yellow powder, mp. 139-141°C; yield 23 %; ^{1}H-NMR (300 MHz; DMSO-d_6) δ: 1.76 (def.t, 2H, SCH_2CH_2), 2.02 (def.t, 2H, NCH_2CH_2), 3.14 (def.t,

J=5.09 Hz, 2H, SCH_2), 3.72 (t, *J*=4.61 Hz, 2H, NCH_2), 5.17 (s, 2H, CH_2O), 6.95 (s, 1H, ArCH=), 7.08 (dd, *J*=8.20 Hz, *J*=2.56 Hz, 1H, Ar H-4'), 7.34-7.50 (m, 3H, Ar H-5', Ar H-3'', H-5''), 7.52 (m, 1H, Ar H-4''), 7.62 (def.dd, *J*=4.10 Hz, *J*=1.54 Hz, Ar H-6''), 7.75 (d, *J*=7.69 Hz, 1H, Ar H-6'), 7.94 (s, 1H, Ar H-2'); ^{13}C-NMR (75 MHz; $CDCl_3$) δ: 28.14 (CH_2); 30.99 (CH_2); 32.43 (SCH_2); 41.08 (NCH_2); 67.25 (CH_2O); 117.49; 117.85; 125.61; 126.94; 127.69; 129.02; 129.04; 129.41; 129.76; 132.77; 134.52; 135.24; 138.87; 158.57 (ArCH=C); 165.09 (C=O); 169.52 (C=N); IR ν: 1725(C=O), 1652(ArCH=), 1576(C=N), 1486, 1374, 1198, 1160, 1027, 967, 756, 650; R_f = 0.76; t_R = 8.56; purity 97.80%; MS calcd for $[M+H]^+$: $C_{21}H_{19}N_2O_2ClS$ m/z: 398.9, found 399.2; CC (CH_2Cl_2 : AcOEt 1 : 1); Anal. Calcd: C 63.22, H 4.80, N 7.02, S 8.04; Found: C, 63.54, H 5.05, N 6.77, S 8.02.

(*Z*)-2-(3-(4-Fluorobenzyloxy)benzylidene)-5,6,7,8-tetrahydroimidazo[2,1-*b*][1,3]thiazepin-3(2*H*)-one (47) Product **47** was purified by column chromatography; yellow powder, mp. 130-133°C (acetonitrile, dioxane); yield 13 %; ^{1}H-NMR (300 MHz; DMSO-d_6) δ: 1.76 (def.t, 2H, SCH_2CH_2), 2.01 (def.t, 2H, NCH_2CH_2), 3.14 (def.t, *J*=5.38 Hz, 2H, SCH_2), 3.72 (t, *J*=4.87 Hz, 2H, NCH_2), 5.09 (s, 2H, CH_2O), 6.93 (s, 1H, ArCH=), 7.05 (dd, *J*=8.20 Hz, *J*=2.17 Hz, 1H, Ar H-4'), 7.20 (t, *J*=8.97 Hz, *J*=2.05 Hz, 2H, Ar H-2'', H-6''), 7.34 (t, *J*=8.75 Hz, 1H, Ar H-5'), 7.50-7.54 (m, 2H, Ar H-3'', H-5''), 7.72 (d, *J*=7.95 Hz, 1H, Ar H-6'), 7.91 (s, 1H, Ar H-2'); ^{13}C-NMR (75 MHz; $CDCl_3$) δ: 28.14 (CH_2); 30.92 (CH_2); 31.01 (SCH_2); 32.44 (NCH_2); 41.07 (CH_2O); 69.36; 115.32; 115.61; 117.23; 117.94; 125.67; 127.74; 129.59; 129.69; 132.59; 135.21; 138.90; 158.64 (ArCH=C); 164.14; 164.98 (C=O); 169.55 (C=N); IR ν: 1705(C=O), 1632(ArCH=), 1570(C=N), 1509, 1494, 1292, 1253, 1221, 1154, 1037, 781, 550; R_f = 0.61; t_R = 8.05; purity 98.01%; MS calcd for $[M+H]^+$: $C_{21}H_{19}N_2O_2FS$ m/z: 382.4, found 383.2; Anal. Calcd: C 65.93, H 5.02, N 7.32, S 8.38; Found: C, 65.66, H 4.89, N 7.02, S 8.11.

Retroviral transfection. CHO K1 cells stably transfected with the human CB_1 and CB_2 receptor were generated with a retroviral transfection system as previously described.[44]

Membrane preparations for CB receptor radioligand binding assays. Frozen rat brains were purchased from Pel Freez®, Rogers, AR, USA. Rat brain cortical membrane preparations were obtained as previously described[52] with minor modifications. Brains were thawed and then kept on ice while the cortex was dissected. The cortex was subsequently homogenized in ice-cold 0.32 M sucrose solution using an Ultra-Turrax® T25 basic homogenizer (IKA Labortechnik) for 10 s at setting 3. The suspension was centrifuged at 1,000 g for 5 min (4°C), the pellet was discarded and the supernatant was subsequently centrifuged at 37,000 g for 60 min (4°C). The supernatant was discarded and the pellet was resuspended in ice-cold water, homogenized with the Ultra Turrax® and recentrifuged at 37,000 g for 60 min (4°C). The resulting membrane pellet was resuspended in Tris-HCl buffer, 50 mM, pH 7.4, and stored at -80°C. Protein concentration was determined by the method of Lowry.[53] Membrane preparations of human embryonic kidney (HEK) 293 EBNA cells expressing the human CB_1, or the human CB_2 receptor, respectively, were obtained from Perkin Elmer, Boston, USA.

Radioligand binding assays at CB_1 and CB_2 receptors. Competition binding assays were performed versus CB agonist radioligand [^{3}H](-)-*cis*-3-[2-hydroxy-4-(1,1-dimethylheptyl)phenyl]-*trans*-4-(3-hydroxypropyl)cyclohexanol (CP55,940) (final concentration 0.1 nM) using rat brain cortical membrane preparations as a source for CB_1 and membrane preparations of human embryonic kidney (HEK293, 50 µg of protein/vial)) cells stably expressing the human receptor subtype (50 µg of protein/vial) as a source for CB_2 receptors. Selected compounds were additionally tested at human CB_1 receptors (50 µg of protein/vial) expressed in HEK293 cells.
The assay was performed as described elsewhere.[44] Stock solutions of the test compounds were prepared in DMSO. The final DMSO concentration in the assay was 2.5%. Data were obtained from at least three independent experiments, performed in duplicates. Data were analyzed using Graph Pad Prism Version 4.02 (San Diego, CA, USA). For the calculation of K_i values the Cheng-Prusoff equation and a K_D value of 2.4 nM ([^{3}H]CP55,940 at hCB_1) and 0.7 nM ([^{3}H]CP55,940 at hCB_1) were used.

[^{35}S]GTPγS binding assays. Assays were performed essentially as previously described.[54] Membrane preparations of rat brain cortical membranes, or commercially available membrane preparations expressing the human CB_1 or CB_2 receptor, respectively, 5 µg per tube, were incubated with 0.1 nM [^{35}S]GTPγS (46.3 TBq/mmol, PerkinElmer Life Sciences, Roddgau-Jügesheim, Germany) in a total volume of 200 µl of Tris-HCl buffer, 50 mM, pH 7.4, containing 1 mM EDTA, 5 mM $MgCl_2$, 1 mM dithiothreitol, 30 µM GDP, 100 mM NaCl, 0.5% bovine serum albumine, and test compound dissolved in DMSO. The final DMSO concentration in the assay was 1%. Nonspecific binding was determined in the presence of 30 µM of unlabeled GTPγS. Incubations were terminated after 60 min of incubation at rt by the addition of 2 ml of ice-cold buffer containing 50 mM Tris-HCl, pH 7.4, and 5 mM $MgCl_2$, and rapid filtration through GF/B glass fiber filter (Schleicher and Schuell, Germany) on a Brandel® 48-channel harvester, followed by two washing steps with ice-cold buffer, 2 ml each. Radioactivity on the wet filters was measured by liquid scintillation counting after punching out the filters and incubating them for 9 h in 2.5 ml of scintillation cocktail (Ready Safe™, Beckman Coulter, USA).

cAMP accumulation assays. Cyclic AMP levels were determined in CHO cells stably expressing the human CB_1 or the human CB_2 receptor subtype, respectively, using a competition binding assay for cAMP according to the procedure described elsewhere.[44] The cAMP binding protein was obtained from bovine adrenal cortex as previously described.[55] Three seperate experminets were performed in duplicates. All data were analyzed with GraphPad Prism, Version 4.02 (GraphPad Inc., La Jolla, CA).

β-Arrestin recruitment assays. Recruitment of β-arrestin molecules to the respective receptor was detected by using β-galactosidase enzyme fragment complementation technology (β-arrestin PathHunter™ assay, DiscoverX, Fremont, CA, USA) as previously described.[28, 40, 42] Data were obtained from three independent experiments, performed in duplicates. Data were analyzed using Graph Pad Prism Version 4.02 (San Diego, CA, USA).

Abbreviations
BTEA, benzyl triethylammonium chloride; CB, cannabinoid; CHO cells, Chinese hamster ovary cells; GPCR, G protein-coupled receptor; GPR18, G protein-coupled receptor 18; GPR55, G protein-coupled receptor 55; HEK cells, human embryonic kidney cells; LPI, lysophosphatidylinositol; MAP kinase, mitogen-activated protein kinase; NAGly, *N*-arachidonoylglycine; nd, not determined; PSB, Pharmaceutical Sciences Bonn; SARs, structure-activity relationships; THC, tetrahydrocannabinol.

Acknowledgements

C.E.M. and K.K.-K. were supported by the Deutscher Akademischer Austauschdienst (DAAD, PPP project). T.K. received a DAAD grant for a research stay in Bonn. C.E.M. and V.R. were funded by the German Federal Ministery for Education and Research (BMBF 01EW0911) in the frame of ERA-NET NEURON. K.K. was supported by a grant from the Polish Ministry of Education and Information, grant No K/ZDS/001915.

Notes and references

[#]PharmaCenter Bonn, Pharmaceutical Institute, Pharmaceutical Chemistry I, An der Immenburg 4, D-53121 Bonn, Germany
[§]Department of Technology and Biotechnology of Drugs, Jagiellonian University Medical College, Faculty of Pharmacy, Kraków, Poland
*To whom correspondence should be addressed: Christa Müller, PharmaCenter Bonn, Pharmaceutical Institute, Pharmaceutical Chemistry I, An der Immenburg 4, D-53121 Bonn, Germany. Phone: +49-228-73-2301. Fax: +49-228-73-2567. E-mail: christa.mueller@uni-bonn.de.

Electronic Supplementary Information (ESI) available: Screening results for agonistic activity in β-arrestin recruitment assays (GPR18, GPR55). K_i values for the compounds at rat CB_1 receptors determined at rat brain cortical membrane preparations. Results from GTPγS binding studies of selected compounds at native rat cannabinoid CB_1 receptors and human cannabinoid CB_1 receptors. Effects of selected compounds on forskolin-induced cAMP accumulation performed with CHO cells stably expressing human CB1 or CB2 receptors. Screening results of selected compounds at GPR35 and the benzodiazepine binding site of $GABA_A$ receptors.

1 H. You, V. M. Gadotti, R. R. Petrov, G. W. Zamponi and P. Diaz, *Mol. Pain*, 2011, **7**, 89.
2 C. M. Henstridge, *Pharmacology*, 2012, **89**, 179-187.
3 F. R. Kreitzer and N. Stella, *Pharmacol. Ther.*, 2009, **122**, 83-96.
4 K. Mackie, *Annu. Rev. Pharmacol. Toxicol.*, 2006, **46**, 101-122.
5 P. Pacher, S. Batkai and G. Kunos, *Pharmacol. Rev.*, 2006, **58**, 389-462.
6 A. Behrenswerth, N. Volz, J. Torang, S. Hinz, S. Bräse and C. E. Müller, *Biorg. Med. Chem.*, 2009, **17**, 2842-2851.
7 A. Kapur, P. Zhao, H. Sharir, Y. Bai, M. G. Caron, L. S. Barak and M. E. Abood, *J. Biol. Chem.*, 2009, **284**, 29817-29827.
8 S. P. Alexander, *Br. J. Pharmacol.*, 2012, **165**, 2411-2413.
9 L. Console-Bram, J. Marcu and M. E. Abood, *Prog. Neuropsychopharmacol. Biol. Psychiatry*, 2012, **38**, 4-15.
10 D. McHugh, *Br. J. Pharmacol.*, 2012, **167**, 1575-1582.
11 D. McHugh, J. Page, E. Dunn and H. B. Bradshaw, *Br. J. Pharmacol.*, 2012, **165**, 2414-2424.
12 M. Kohno, H. Hasegawa, A. Inoue, M. Muraoka, T. Miyazaki, K. Oka and M. Yasukawa, *Biochem. Biophys. Res. Commun.*, 2006, **347**, 827-832.
13 D. McHugh, S. S. Hu, N. Rimmerman, A. Juknat, Z. Vogel, J. M. Walker and H. B. Bradshaw, *BMC Neurosci.*, 2010, **11**, 44.
14 Y. Qin, E. M. Verdegaal, M. Siderius, J. P. Bebelman, M. J. Smit, R. Leurs, R. Willemze, C. P. Tensen and S. Osanto, *Pigment Cell Melanoma Res.*, 2011, **24**, 207-218.
15 A. J. Brown, D. A. Daniels, M. Kassim, S. Brown, C. P. Haslam, V. R. Terrell, J. Brown, P. L. Nichols, P. C. Staton, A. Wise and S. J. Dowell, *J. Pharmacol. Exp. Ther.*, 2011, **337**, 236-246.
16 C. M. Henstridge, N. A. Balenga, R. Schröder, J. K. Kargl, W. Platzer, L. Martini, S. Arthur, J. Penman, J. L. Whistler, E. Kostenis, M. Waldhoer and A. J. Irving, *Br. J. Pharmacol.*, 2010, **160**, 604-614.
17 C. M. Henstridge, N. A. Balenga, L. A. Ford, R. A. Ross, M. Waldhoer and A. J. Irving, *FASEB J.*, 2009, **23**, 183-193.
18 R. Pineiro, T. Maffucci and M. Falasca, *Oncogene*, 2011, **30**, 142-152.
19 E. Ryberg, N. Larsson, S. Sjogren, S. Hjorth, N. O. Hermansson, J. Leonova, T. Elebring, K. Nilsson, T. Drmota and P. J. Greasley, *Br. J. Pharmacol.*, 2007, **152**, 1092-1101.
20 L. S. Whyte, E. Ryberg, N. A. Sims, S. A. Ridge, K. Mackie, P. J. Greasley, R. A. Ross and M. J. Rogers, *Proc. Natl. Acad. Sci. U. S. A.*, 2009, **106**, 16511-16516.
21 R. A. Ross, *Trends Pharmacol. Sci.*, 2011, **32**, 265-269.
22 H. Sharir and M. E. Abood, *Pharmacol. Ther.*, 2010, **126**, 301-313.
23 S. Anavi-Goffer, G. Baillie, A. J. Irving, J. Gertsch, I. R. Greig, R. G. Pertwee and R. A. Ross, *J. Biol. Chem.*, 2012, **287**, 91-104.
24 H. B. Bradshaw, N. Rimmerman, S. S. Hu, V. M. Benton, J. M. Stuart, K. Masuda, B. F. Cravatt, D. K. O'Dell and J. M. Walker, *BMC Biochem.*, 2009, **10**, 14.
25 V. B. Lu, H. L. Puhl, 3rd and S. R. Ikeda, *Mol. Pharmacol.*, 2013, **83**, 267-282.
26 H. Yin, A. Chu, W. Li, B. Wang, F. Shelton, F. Otero, D. G. Nguyen, J. S. Caldwell and Y. A. Chen, *J. Biol. Chem.*, 2009, **284**, 12328-12338.
27 S. Heynen-Genel, R. Dahl, S. Shi, L. Milan, S. Hariharan, E. Sergienko, M. Hedrick, S. Dad, D. Stonich, Y. Su, M. Vicchiarelli, A. Mangravita-Novo, L. H. Smith, T. D. Y. Chung, H. Sharir, M. G. Caron, L. S. Barak and M. E. Abood, *Probe Reports from the NIH Molecular Libraries Program*, 2010, 1-26.
28 V. Rempel, N. Volz, F. Glaser, M. Nieger, S. Bräse and C. E. Müller, *J. Med. Chem.*, 2013, **56**, 4798-4810.
29 U. Geis, K. Kieć-Kononowicz and C. E. Müller, *Sci. Pharm.*, 1996, **64**, 383-390.
30 J. Karolak-Wojciechowska and K. Kieć-Kononowicz, *Journal of Crystallographic and Spectroscopic Research*, 1987, **17**, 485-494.
31 J. Karolak-Wojciechowska, M. Mikołajczyk, A. Zatorski, A. Zejc and K. Kieć-Kononowicz, *Tetrahedron*, 1985, **41**, 4593-4602.
32 K. Kieć-Kononowicz and J. Karolak-Wojciechowska, *Phosphorus, Sulfur, Silicon*, 1992, **73**, 235-248.
33 K. Kieć-Kononowicz, J. Karolak-Wojciechowska, B. Michalak, E. Pękala, B. Schumacher and C. E. Müller, *Eur. J. Med. Chem.*, 2004, **39**, 205-218.
34 K. Kieć-Kononowicz, J. Karolak-Wojciechowska, C. E. Müller, B. Schumacher, E. Pękala and E. Szymanska, *Eur. J. Med. Chem.*, 2001, **36**, 407-419.
35 K. Kieć-Kononowicz, C. E. Müller, E. Pękala, J. Karolak-Wojciechowska, J. Handzlik and D. Łażewska, *J. Heterocycl. Chem.*, 2002, **39**, 243–253.
36 K. Kieć-Kononowicz, A. Zatorski and J. Karolak-Wojciechowska, *Phosphorus, Sulfur, Silicon*, 1989, **42**, 191-200.

37 K. Kieć-Kononowicz, A. Zejc, M. Mikołajczyk, A. Zatorski, J. Karolak-Wojciechowska and M. W. Wieczorek, *Tetrahedron*, 1980, **36**, 1079-1087.
38 K. Kieć-Kononowicz, A. Zejc, M. Mikołajczyk, A. Zatorski, J. Karolak-Wojciechowska and M. W. Wieczorek, *Tetrahedron*, 1981, **37**, 409-415.
39 M. Funke, D. Thimm, A. C. Schiedel and C. E. Müller, *J. Med. Chem.*, 2013, **56**, 5182-5197.
40 V. Rempel, A. Fuchs, S. Hinz, T. Karcz, M. Lehr, U. Koetter and C. E. Müller, *ACS Med. Chem. Lett.*, 2013, **4**, 41-45.
41 C. Southern, J. M. Cook, Z. Neetoo-Isseljee, D. L. Taylor, C. A. Kettleborough, A. Merritt, D. L. Bassoni, W. J. Raab, E. Quinn, T. S. Wehrman, A. P. Davenport, A. J. Brown, A. Green, M. J. Wigglesworth and S. Rees, *J. Biomol. Screen.*, 2013, **18**, 599-609.
42 D. Thimm, M. Funke, A. Meyer and C. E. Müller, *J. Med. Chem.*, 2013, **56**, 7084-7099.
43 R. G. Pertwee, A. C. Howlett, M. E. Abood, S. P. Alexander, V. Di Marzo, M. R. Elphick, P. J. Greasley, H. S. Hansen, G. Kunos, K. Mackie, R. Mechoulam and R. A. Ross, *Pharmacol. Rev.*, 2010, **62**, 588-631.
44 V. Rempel, N. Volz, S. Hinz, T. Karcz, I. Meliciani, M. Nieger, W. Wenzel, S. Bräse and C. E. Müller, *J. Med. Chem.*, 2012, **55**, 7967-7977.
45 E. Cichero, A. Ligresti, M. Allara, V. di Marzo, Z. Lazzati, P. D'Ursi, A. Marabotti, L. Milanesi, A. Spallarossa, A. Ranise and P. Fossa, *Eur. J. Med. Chem.*, 2011, **46**, 4489-4505.
46 E. Kotsikorou, K. E. Madrigal, D. P. Hurst, H. Sharir, D. L. Lynch, S. Heynen-Genel, L. B. Milan, T. D. Chung, H. H. Seltzman, Y. Bai, M. G. Caron, L. Barak, M. E. Abood and P. H. Reggio, *Biochemistry (Mosc).* 2011, **50**, 5633-5647.
47 M. G. Schmeisser, E. A. Pearsall and P. H. Reggio, *Biophys. J.*, 2013, **104**, 409A.
48 R. G. Pertwee, *AAPS J.*, 2005, **7**, E625-654.
49 C. S. Breivogel, D. E. Selley and S. R. Childers, *J. Biol. Chem.*, 1998, **273**, 16865-16873.
50 R. S. Landsman, T. H. Burkey, P. Consroe, W. R. Roeske and H. I. Yamamura, *Eur. J. Pharmacol.*, 1997, **334**, R1-2.
51 P. Zhao and M. E. Abood, *Life Sci.*, 2013, **92**, 453-457.
52 L. Yan and C. E. Müller, *J. Med. Chem.*, 2004, **47**, 1031-1043.
53 O. H. Lowry, N. J. Rosebrough, A. L. Farr and R. J. Randall, *J. Biol. Chem.*, 1951, **193**, 265-275.
54 A. Thomas, L. A. Stevenson, K. N. Wease, M. R. Price, G. Baillie, R. A. Ross and R. G. Pertwee, *Br. J. Pharmacol.*, 2005, **146**, 917-926.
55 C. Nordstedt and B. B. Fredholm, *Anal. Biochem.*, 1990, **189**, 231-234.

TOC Graphic